Miro Aalto

Application of Weather Data in the Abatement of Impulse Noise

School of Electrical Engineering

Thesis submitted for examination for the degree of Master of Science in Technology.

Espoo 20.08.2015

Thesis supervisor:

Prof. Ville Pulkki

Thesis advisors:

M.Sc (Tech) Timo Peltonen

M.Sc (Tech) Timo Markula

Aalto University
School of Electrical
Engineering

AALTO-YLIOPISTO
SÄHKÖTEKNIIKAN KORKEAKOULU

DIPLOMITYÖN
TIIVISTELMÄ

Tekijä: Miro Aalto

Työn nimi: Säätietojen hyödyntäminen impulssimaisen melun torjunnassa

Päivämäärä: 20.08.2015 Kieli: Englanti Sivumäärä: 8+67

Akustiikan ja signaalinkäsittelyn laitos

Professuuri: S.89

Työn valvoja: Prof. Ville Pulkki

Työn ohjaajat: M.Sc (Tech) Timo Peltonen, M.Sc (Tech) Timo Markula

Ääni, joka koetaan häiritseväksi tai on haitallista ihmiselle, on määritelty meluksi. Nykypäivän ympäristössä on useita melunlähteitä ja niiden aiheuttamat äänet kulkeutuvat asuintaloihin sekä työpaikoille vaikuttaen myös terveyteemme. Taajuusalue, jonka ihminen kykenee kuulemaan käsittää 20Hz...20kHz taajuuskaistan. Eri taajuiset ääniaallot vaimenevat eri tavoin edetessään ilmakehässä pitkiä matkoja, ja esimerkiksi pienet taajuudet vaimenevat vähemmän pitkillä matkoilla sekä kykenevät tunkeutumaan seinien läpi paremmin verrattuna suuriin taajuuksiin.

Tässä opinnäytetyössä käsitellään räjäytysten aiheuttaman pienitaajuisen melun etenemistä ulkoilmassa. Erityisen tarkastelun alla ovat eri sääolosuhteiden vaikutukset äänen etenemiseen ja tarkastelun työkaluina käytetään mittauksia sekä melumallinnuksia. Mittaukset on tehty yhteistyössä Puolustusvoimien Räjähdekeskuksen kanssa Ähtärin Palolammen hävittämöllä, jolla sijaitsee myös tutkimuksissa hyödynnettävä sääasema.

Tutkimuksssa esiintyvät mittaukset sekä mallinnukset antoivat yhteneviä tuloksia sään vaikutuksista äänen etenemiseen. Suurin merkitys oli melun etenemisuunnan kanssa yhdensuuntaisella tuulennopeuskomponentilla, joka aiheuttaa äänelle suotuisat tai epäsuotuisat etenemisolosuhteet. Mallinnuksien tulokset olivat linjassa mittausten kanssa, mutta mallinnettujen ja mittauksissa havaittujen äänialtistustasojen välillä oli merkittäviä eroja. Mallinnus antoi suurempia tasoja vastatuuleen ja pienempiä tasoja myötätuuleen. Näitä havaintoja voidaan käyttää hyödyksi räjäytyksistä aiheutuvien meluhaittojen arvioinnissa sekä minimoinnissa.

Avainsanat: melu, ympäristömelu, impulssi, räjähdys, sääolosuhteet

AALTO UNIVERSITY
SCHOOL OF ELECTRICAL ENGINEERING

ABSTRACT OF THE
MASTER'S THESIS

Author: Miro Aalto

Title: Application of weather data in the abatement of impulse noise

Date: 20.08.2015 Language: English Number of pages: 8+67

Department of Acoustics and Signal Processing

Professorship: S.89

Supervisor: Prof. Ville Pulkki

Advisor: M.Sc Timo Peltonen & M.Sc Timo Markula

Noise is defined as sound that causes harm or annoyance to people. In modern environment, there are numerous sources of noise around our habitat. Traffic, power plants and construction yards can be seen as noise sources as they cause different kinds of sounds that can disturb our work or penetrate the walls of the living premises, affecting our health. Within generally accepted audible range, noise can contain frequencies between 20Hz and 20kHz. Low frequencies tend to penetrate facades better than higher frequencies, and they also propagate longer distances outdoors.

In this thesis the outdoor diffusion of low frequency noise caused by explosives is being studied by measurements and predictive calculation models. The focus is kept in meteorological conditions and their effects on sound propagation. The measurements have been conducted in co-operation with Finnish Defence Forces at their explosives demolition center that has an onsite meteorological station.

Measurements and predictive calculations showed similar results: the meteorological conditions have a clear effect on sound propagation. The dominant parameter was the wind component parallel to the propagation path and a clear correlation was found. The predictive calculations gave similar results compared to measurements, even though the difference under the modeled conditions showed higher sound exposure levels under upwind propagation conditions and lower levels under downwind conditions. In order to minimize the noise immissions caused by demolition activity, the results can be utilized in the assessment of impulse noise.

Keywords: noise, environmental noise, weather conditions, explosions, impulse noise, noise abatement

Acknowledgements

This project was carried out in co-operation with Akukon Oy and Finnish Defense Forces and I want to express my gratitude to these two organizations for providing this opportunity.

I would like to thank all the co-workers in Akukon and especially my instructors Timo Peltonen and Timo Markula for guidance and support through the project. I am also grateful to Asko Parri from Finnish Defense Forces and the whole crew in Ähtäri for being flexible and helpful when I suffered some major setbacks.

I also wish to thank Professor Ville Pulkki for supervising this thesis and giving valuable feedback.

In the end, I want to thank my family and friends for the support throughout this longish journey.

Otaniemi, 20.08.2015

Miro Aalto

Contents

Symbols and abbreviations

Symbols

dB	Decibel
L_w	Sound power level (dB re 1pW)
L_p	Sound pressure level (dB re 20μPa)
L_{eq}	Equivalent continuous sound pressure level
p	Pressure
p_0	Reference sound pressure (dB 20μPa)
P_0	Reference sound power (1pW = 10^{-12}W)
W	Power (watts)
ρc	Characteristic specific acoustic impedance
I	Intensity
I_0	Reference intensity ($1\frac{pW}{m^2}$)
L_i	Sound intensity level (dB re $1\frac{pW}{m^2}$)
L_J	Sound energy level (dB re 1pJ)
J_o	Reference sound energy level (10pJ)
L_E	Sound exposure level (dB re $400(\mu Pa)^2$s)
E_0	Reference sound exposure ($400(\mu Pa)^2$s)
c	Speed of sound ($\frac{m}{s}$)
f	Frequency (Hz)
ω	Angular frequency ($\frac{rad}{s}$)
ϕ	Phase (radians)
T	Absolute emperature (K)
t	Temperature in celsius (°C)
$^\circ C$	degrees Celsius
λ	Wavelength (m)
M	Molecular weight ($\frac{kg}{mol}$)
R	Molar gas constant (approximately $8.3145 J \cdot mol^{-1} \cdot K^{-1}$)
γ	Adiabatic index (constant)
F, S, I	Time weightings (Fast, Slow, Impulse)
Z, C, A	Frequency weightings (linear, C, A)
k	The Boltzmann constant ($1.3806488{\cdot}10^{-23}\frac{J}{K}$)
R	Reflection coefficient
Z	Ground impedance
σ	Flow resistivity ($\frac{Ns}{m^4}$)

Abbreviations

FDF	Finnish Defence Forces (Suomen Puolustusvoimat)
RÄJK	Räjähdekeskus
B&K	Brüel & Kjaer
LF	Low Frequency
SPL	Sound Pressure Level
TNT	Trinitrotoluene
GPM	General Prediction Method
R.E	Relative Efectiveness Factor
TG	Temperature Gradient
W	Wind Component
FIR	Finite Impulse Response
IIR	Infinite Impulse Response
FFT	Fast Fourier Transform

1 Introduction

1.1 Background

Räjähdekeskus (RÄJK) is a part of Finnish Defence Forces (FDF). Their area of responsibility is to produce, maintain and dispose explosives. The latter one generates substantial amounts of noise into the environment and people living near by have complained about it.

Now RÄJK has recently acquired a meteorological station with sensors mounted onto a 40 meter high mast. With this equipment it is possible to measure several important quantities like wind speed, wind direction and temperature at different heights. These weather parameters are known to have an impact on sound propagation at long distances [1, 2].

1.2 Objectives

The purpose of this thesis is to study measured weather data for predicting the attenuation and levels of impulsive noise from open air blasting under different weather conditions, direction and distances from the site. The study includes a series of noise measurements made onsite at a representative distance from the noise source. This work aims at building a novel noise abatement strategy for Finnish Defence Forces. The main questions to be investigated are:

- How do meteorological conditions affect the propagation of low frequency noise at long distances (several kilometers)?
- Can the meteorological station be utilized in finding favorable and unfavourable sound propagation conditions in order to avoid noise complaints?
- Possibilities to apply the results to similar activities in FDF's actions.

In this thesis the basic concepts of sound and noise are introduced, and environmental sound propagation mechanisms are studied in theory and by computational models. The results from noise models are compared to the conducted measurements, with cross-checking the recorded data from the meteorological station.

2 Noise and sound

2.1 Basic concepts

In air, sound can be considered as pressure changes around the atmospheric pressure, propagating as waves and attenuating in distance. There are several mechanisms that can act as a source of sound, in [4] they are listed as follows:

- Vibrating bodies: for example a vibrating string causing local pressure changes as a result of air displacement next to it
- Changing airflow: vocal folds open and close change the airflow rate from lungs when e.g. speaking
- Time-dependent heat sources: An explosion heating the air rapidly and causing its expansion
- Supersonic flow: An object like bullet forcing air to flow faster than the speed of sound resulting as a shock wave

2.1.1 Physical quantities

Sound pressure

The pressure changes that can be perceived as an audible sound are relatively small compared to static atmosphere. In general the range human hearing is capable to process is around 20μPa...20Pa and the lower limit, $p_0 = 20\mu$Pa, is defined as the reference sound pressure, the threshold of hearing.

The pressure changes can be converted into electrical form (voltage signal) with an electro acoustical transducer like microphone. The pressure can now be expressed as function of time t as follows:

$$p(t) = \hat{p}\sin(\omega t + \phi), \tag{1}$$

where $\hat{p}$ is the amplitude, $\omega = 2\pi f$ is the angular speed with frequency f, and ϕ is the phase.

From this the root-mean-squared (RMS) sound pressure $\tilde{p}$ can be obtained by taking the squared average over time:

$$\tilde{p} = \sqrt{\frac{1}{T}\int_0^T p^2(t)dt}. \tag{2}$$

Sound power and intensity

As *mechanical work* can be defined by a force F multiplied by velocity vector v, the total acoustical energy flow through a surface element $\vec{S}$ can be defined in the same manner using the sound pressure p and the particle velocity $\vec{u}$:

$$E = \int_{-\infty}^{\infty} \int_S p(t)\vec{u}(t) \cdot d\vec{S}dt. \tag{3}$$

Now the transient sound power P, the rate of acoustical energy flow radiated from the source through a surface S, can be defined as

$$P(t) = \int_S \vec{I}(t) \cdot d\vec{S}, \tag{4}$$

where

$$\vec{I}(t) = p(t)\vec{u}(t) \tag{5}$$

is the sound intensity $\vec{I}$ as a function of time. In general, without time dependence, the sound intensity I through a surface area S perpendicular to surface normal is

$$I = \frac{P}{S}. \tag{6}$$

Frequency content

As sound results from vibrations (repeating events), it contains also frequency information. The basic definition of frequency (f) is determined by n repeating events per second ($f = \frac{n}{t}$) and its unit is *hertz* (Hz). The frequency of a sound wave also depends on the speed of sound (c) in the medium and the wavelength (λ) of the pressure wave:

$$f = \frac{c}{\lambda}. \tag{7}$$

The audible range for human hearing is 20Hz...20000Hz. Sounds below 20Hz are called *infrasounds* and sounds exceeding the human hearing are called as *ultrasounds*. [5]

Speed of sound

The speed of sound depends on the properties of the media, for example, the sound wave travels in liquids and different gases at different speed. The general equation [4] for the speed of sound in ideal gas is:

$$c = \sqrt{\frac{\gamma RT}{M}}, \tag{8}$$

where T stands for absolute temperature, M for the molecular weight of the gas, R is the molar gas constant and γ is adiabatic index. To simplify this, in air, the speed of sound can be approximated [4] in different temperatures (T, in celsius) as

$$c = 331.3 + 0.6T. \tag{9}$$

2.1.2 Level quantities

Sound pressure level

Sound pressure changes are most commonly expressed using different level expressions in decibels (dB) due to the logarithmic behavior of the human hearing system [1]. For sound pressure level (SPL) this means the logarithmic root-mean-squared sound pressure in ratio to the reference sound pressure p_0:

$$L_{\mathrm{P}} = 10 \log \left(\frac{\tilde{p}^2}{p_0^2} \right). \tag{10}$$

Sound power level

Sound power level is used to describe the amount of acoustical power produced by a sound source. It can be expressed as follows:

$$L_{\mathrm{W}} = 10 \log \left(\frac{P}{P_0} \right), \tag{11}$$

where P is the measured sound power (in watts) and $P_0 = 1\mathrm{pW}$ is the reference value.

Like the sound reference pressure p_0, also the reference value for sound power level is connected to the threshold of hearing. As described in [1], the sound power of a plane wave propagating in a medium without any interaction with obstacles (i.e. in *free field*) is:

$$W = \frac{p^2}{\rho c}, \tag{12}$$

where ρ is the density of the medium and c the speed of sound. Under normal circumstances the product ρc, also called the *characteristic specific acoustic impedance*, is around $400 \frac{\mathrm{kg}}{\mathrm{m}^2}$. Hence, the sound power of a plane wave with pressure of $20\mu\mathrm{Pa}$ is 1pW.

Sound intensity level

As the sound intensity is a vector quantity describing the sound power per unit area, the sound intensity level describes the acoustic energy flow and is defined by:

$$L_{\mathrm{I}} = 10 \log \left(\frac{|\vec{I}|}{I_0} \right), \tag{13}$$

where $|\vec{I}|$ is the measured intensity perpendicular to surface normal and $I_0 = 1 \frac{\mathrm{pW}}{\mathrm{m}^2}$ is the reference value.

Equivalent continuous sound pressure level

The equivalent sound pressure level is one of the most important level quantities used widely in noise assessment, abatement and legislation. It is tightly connected to the RMS value of sound pressure, which means that the louder sounds will stand out (as the sound pressure is squared) when noise levels are observed. The equivalent sound pressure level L_{eq} is defined as:

$$L_{\mathrm{eq}} = 10\log\left(\frac{1}{T}\int_T \frac{p^2(t)}{p_0^2)}dt\right) = 20\log\sqrt{\frac{1}{T}\int_T \frac{p^2(t)}{p_0^2}dt}, \tag{14}$$

where T is the observation time interval in seconds.

Sound exposure level

Compared to the equivalent sound pressure level L_{eq}, the sound exposure level L_E is used when the noise event is limited in time. This means it can be applied when the objective is to find out how a single noise event or multiple single events (e.g explosions) affect the equivalent level over a certain time period. In the basic form, the sound exposure level L_E is defined as:

$$L_{\mathrm{E}} = 10\log\left(\frac{1}{t_0}\int_T \frac{p^2(t)}{p_0^2}dt\right) = 20\log\sqrt{\frac{1}{t_0}\int_T \frac{p^2(t)}{p_0^2}dt}, \tag{15}$$

where $t_0 = 1$s and T is the time interval of observation. To figure out the equivalent level consisting of multiple single events, the following is used:

$$L_{\mathrm{eq}} = 10\log\left(\sum_{i=1}^{N} 10^{\frac{L_{Ei}}{10}}\right) - 10\log\left(\frac{T}{t_0}\right), \tag{16}$$

Sound energy level

Sound energy level L_J is a property of the sound source, a time limited noise emission of the source. It is defined by the *sound energy* E and the reference sound energy E_0=10pJ (pico-joule) as follows:

$$L_{\mathrm{J}} = 10\log\left(\frac{E}{E_0}\right). \tag{17}$$

The sound energy level L_J is also connected to the sound power level L_W in a similar way like equivalent sound pressure level is connected to the sound exposure level L_E:

$$L_{\mathrm{J}} = L_{\mathrm{W}} + 10\log\left(\frac{T}{t_0}\right), \tag{18}$$

where t_0 =1s and T the length of the event.

2.1.3 Noise annoyance

Sound that is harmful or annoying to people is defined as noise. Annoyance is one of the major issues linked to environmental noise. It is subjective experience, and it is not simple to assess which kind of sound is experienced as noise and by whom. No doubt that some people are disturbed by outdoor events or overflights, or some may enjoy listening to a rock concert in the city area. The field studying how people perceive the sound, or in other words people's sensation in consequence to a stimulus, is called psychoacoustics [5].

Loudness level

It is not a simple task to quantitatively describe (or even measure) annoyance. There are many quantities that can be used to describe annoyance at some level. These quantities are usually results of broad listening tests and they are applied to describe how the auditory system works, one of them is called *loudness*. It describes how loud the sound is perceived.

One of the most common applications of loudness is to utilize standardized (ISO 226:2003 [7]) equal-loudness-level contours (Figure 1) to model the sensitivity of human hearing at different frequencies and levels. The Figure 1 shows that the human hearing is more sensitive at 250Hz...4kHz range than at lower frequencies. The unit of loudness level is *phon*, which is defined as a number equal to the sound pressure level of a tone that is perceived as loud as a 1kHz reference tone with the same sound pressure level [5].

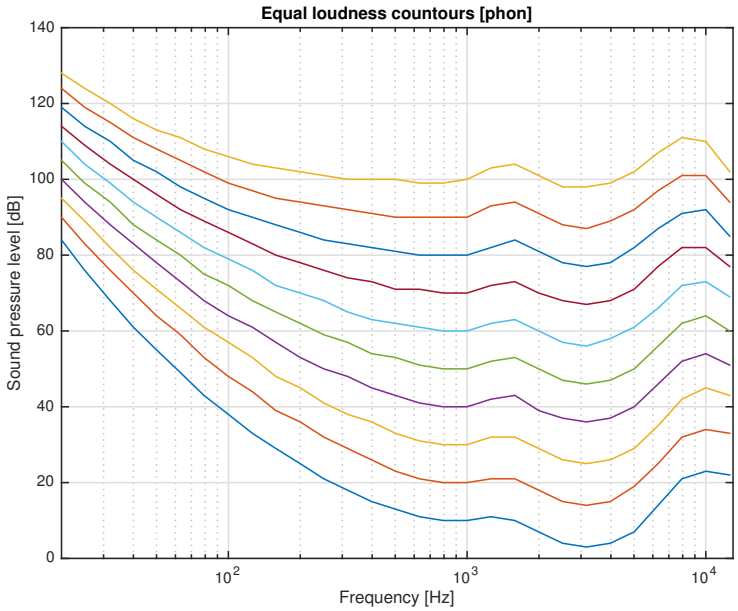

Figure 1: Standardized [7] equal loudness level contours. The loudness level equals to the sound pressure level at 1kHz, for example the first contour line from below corresponds to loudness level of 10 phon.

Frequency weighting

To utilize the knowledge of sensitivity of human hearing, frequency weighting networks are introduced (Figure 2). In practice, a suitable frequency weighting network filter is applied to the measurements in order to approximate how loud the noise will be perceived. Standardized weighting networks used in modern sound level meters are A-, C- and Z-weightings (according to IEC 616721-1:2013 [8]). The A-weighting is the most commonly used in noise measurements, and initially it was designed to model the loudness contours at lower SPLs (<55dB). The C network was originally suggested to be used at higher SPLs (>85dB), but later on, the A-weighting was discovered in practice to be the most accurate network simulating human hearing [1, 9].

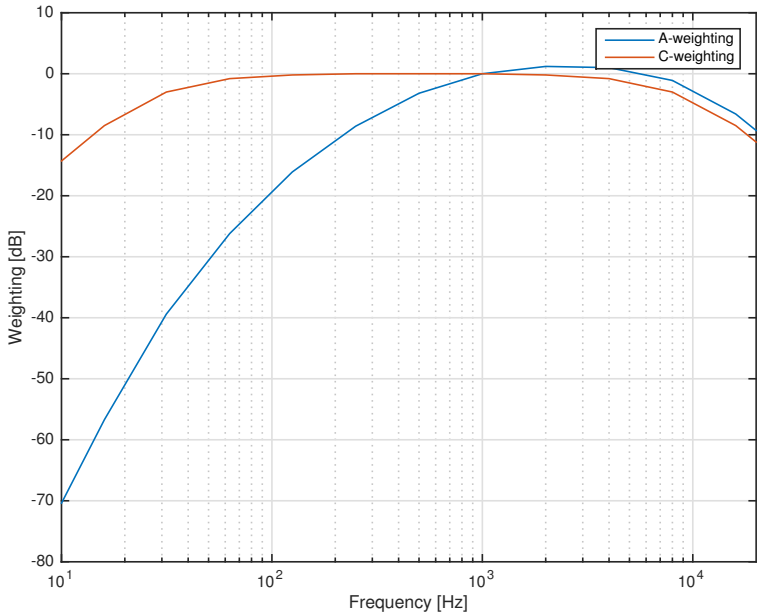

Figure 2: A- and C-weighting curves (10...20000Hz). As can be seen, the A-weighting attenuates the low frequencies more than C-weighting, and follows the loudness level contours especially at low sound pressure levels. The C-weighting was suggested to be used at higher SPLs, but the A-weighting was found to be the most accurate [1].

The Z (zero) or linear weighting, does not include any level correction terms at any frequency and so it does not have an effect on the measured waveform in the audio band. One other common factor between these networks, in addition to the equal-loudness-level contours, is that they all have been normalized to have 0dB correction at 1kHz. The reason for this is practical: the sound level meters are calibrated using a 1kHz tone.

It is noteworthy to mention, that the frequency weighting filters have been criticized due to their tolerances in bandwidth, especially below 20Hz [10]. The tolerances are presented in the sound level meters' specification standard [8]. As

an example, in a sound level meter that fulfills the standard (IEC class 1), at 20Hz band the tolerance is $\pm 2.5dB$. In this case, the error in SPL between two sound level meters can be 5dB (at 20Hz band).

Time weighting

Time weighting is another method to quantify perceived loudness. The perceived loudness grows when the sound duration is increased due to the time it takes for the auditory system to average the sound. This *integration time* is about 100...200ms, and after this loudness does not increase. The studies done back in 1960's show that the level of loudness increases approximately 10dB when the stimulus duration increases by factor of 10, in case of narrow band noise [11]. When it comes to broadband noise, the increment in the loudness level is less faster [4]. On the other hand, with higher SPLs a faster averaging time is reasonable [12].

In (analog) sound level meters, time weighting was applied using different resistor-capcitor (RC) circuits in order to conduct the averaging, or in other words, integration. Nowadays this is implemented digitally. There used to be three standardized [8] weightings: F (fast), S (slow), and I (impulse) weighting. The F time constant is closest to the human hearing integration time. Their corresponding time constants are 125ms (F), 1000ms (S) and 35ms rise time with 1.5s decay time (I). The integration time is two times the time constant for fast and slow weightings, and for impulses, two times the rise time.

Nowadays the impulse weighting has been dropped from the standard due to its insufficiency to fulfill its purpose, not only as a measurement time constant, but also as an indicator to predict hearing damage from impulse noise. Even so, I-weighting is still widely used due to legislation. [1]

2.1.4 Noise guidelines and recommendations

General statutes

As noise is defined and experienced as harmful or disturbing, there are usually noise related legislation and guidelines set by the authorities of a certain country or area. In Finland the following noise guidelines and recommendations are set by Ministry of the Environment (Ympäristöministeriö) in Government Decree on Guidelines on Noise Levels (Valtioneuvoston päätös 993/1992) [13]. The values are presented as A-weighted equivalent levels in Table 1 below. To be noticed, these guidelines exclude e.g. shooting ranges [14] and noise generated by heavy weapons and explosions [15].

Occupational health and safety

The legislation about occupational health and safety for employers is determined in [16]. The possible hearing damage is taken into account in legislation and legislation's translations [17, 18] that also include the indoor and outdoor noise guidelines. The noise guidelines for workplaces are presented in Table 2 below.

Table 1: Guidelines for outdoor/indoor noise levels (L_{Aeq}) according to [13]. This table does not concern neither shooting ranges or motor sport tracks, and it is not applied to traffic or industrial areas. General areas includes residential areas, recreation areas close to population centers, institutions and academies.

Outdoor areas	**Day (07-22)**	**Night (22-07)**
Living-, in suburb recreational areas, nursing and educational institutions	55dB	50dB
Vacation-, camping-, recreational- and conservation areas	45dB	40dB
Indoors		
Residential and hospitals	35dB	30dB
Educational and recreational	35dB	-
Offices	45dB	-

Table 2: Occupational health and safety noise guideline values for workplaces according to [16, 17, 18].

Guideline values	L_{Aeq8h}	L_{Cpeak}	**Note**
Lower value	80dB	135dB	Measured outside of hearing protection
Upper value	85dB	137dB	Measured outside of hearing protection
Off limit	87dB	140dB	Measured inside of hearing protection

The guideline values in Table 2 require certain actions from employer and employee. If the lower guideline value is reached, the employer must provide hearing protection. In case of the upper guideline value, it is mandatory to wear hearing protection. If off limits are reached, the employer must start reducing the noise emissions, at the latest.

Shooting ranges and small calibre weapons

In Table 3 the shooting range activities the noise guideline values are presented according to [14]. Note that, the these guidelines are only intended for shooting ranges and small calibre weapons.

Table 3: Noise guideline values for shooting range activities according to [14]. The quantity to be measured is the outdoor daytime I-weighted maximum A level, L_{AImax}.

Noise guidelines for shooting range activity	L_{AImax}
Residential and educational premises	65dB
Hospitals, vacation homes, nature reserves	60dB

Heavy weapons and explosions

In the Finnish Defense Forces's guidelines for heavy weapon noise [15], heavy weapons are outlined to be all weapons with a caliber over 12.7mm, and explosives or materials containing amounts of explosive agent equivalent to at least 60 grams of trinitrotoluene (TNT).

In heavy weapons noise assessment the first quantity to measure is the C-weighted peak level, L_{Cpeak}. In Finland, it is used to evaluate the threats of impulsive noise in occupational health and safety. Despite of the fact that L_{Cpeak} is primarily intended for the assessment of hearing damage, it is also used in environmental noise assessment. In addition, a study results about the annoyance and the outdoor peak levels L_{Cpeak} are put together in [15] and presented presented in Table 4.

Table 4: The annoyance of different C peak levels according to [15].

Annoyance	**Average** L_{Cpeak}	**Variation** L_{Cpeak}
Not all	107dB	100-115dB
A little	108dB	100-115dB
More than a little	112dB	106-123dB
A lot	116dB	110-127dB
Very much	123dB	115-130dB

As covered later, noise generated by the activities in question has a remarkable low frequency content. This justifies the use of C-weighting for the evaluation of environmental noise caused by explosion and perceived inside buildings.

As mentioned, the limit for hearing damages is assumed to be $L_{\mathrm{Cpeak}} = 140$dB. Even so, for the assessment of environmental noise, a single peak level or average of multiple noise events is not enough. This is due to fact that peak levels do not illustrate the daily total noise levels caused by e.g. multiple detonations per day or in a row.

The C-weighted sound exposure level, L_{CE}, is used for the evaluation of noise exposure caused by a single noise event. This is a common convention also in the other Nordic countries and e.g. in USA. [18]

The outdoor noise levels brought on by heavy weapons or explosions should not exceed the $L_{\mathrm{Cpeak}} \leq 115$dB guideline value at residential areas. In case of exceeded peak levels, the C-weighted sound exposure and A-weighted daytime equivalent level measurements are needed in order to assess the environmental noise emissions in the area of interest. The limit for the L_{CE} is 100dB and the guideline value for the daytime equivalent level $L_{\mathrm{Aeq,d}}$ is 55dB (based on [13]). The penalty, correction, for impulsive noise is a 9dB increment for the measured or calculated noise levels if a more accurate value is not proposed. [15]

2.2 Outdoor sound propagation

In an ideal medium in a free field, sound spreads from a point source as a spherical wave in every direction without interaction with obstacles, but in practice this does not occur without a number of other factors. The atmosphere absorbs sound energy and can bend the sound waves, obstacles induce attenuation, scattering and diffraction, and the ground reflects the sound causing phase differences between incoming waves at the receiver. These factors must be taken into account when calculating or predicting noise propagation outdoors.

2.2.1 Divergence

In order to form sound or noise, a sound source is needed. As mentioned earlier, the sound power is defined as the rate of energy flow radiated from a source through a surface area. In the case of an ideal sound (point) source, the energy radiates evenly in every direction through a spherical surface S with radius r ($S_{\text{sphere}} = 4\pi r^2$), centered at the source. Thus Equation 6 can be expressed as

$$I = \frac{P}{4\pi r^2}. \tag{19}$$

As the sound wave is in motion, the surface expands and its area grows in relation to the radius squared. This gives us the attenuation (in dB) in relation to the distance from the sound source:

$$A_{\text{d}} = 10 \log \left(\frac{1}{4\pi r^2} \right). \tag{20}$$

It is noteworthy that in this thesis the explosive material is often placed directly on the ground and thus the expanding surface is seen as hemisphere ($S_{hemisphere} = 2\pi r^2$). When observed from a longer distance, a spherical point source can be used as an approximation as ground reflection is taken into account.

2.2.2 Ground effect

Another important factor in sound propagation is the ground reflection between the source and the receiver. Absorption and reflection may induce attenuation or amplification in the sound levels depending on the distance to the source. This is due to the phase differences, or in other words, constructive or destructive interference between the direct and reflected sound at the point of interest. The ground borne interference occurs due to the following factors:

- The reflected path of the sound is longer than the direct path
- The ground is rarely perfectly reflecting, i.e. it has a finite impedance

The ground reflection (Figure 3) can be approximated using the superposition of two pressure waves:

$$p_{\text{tot}} = p_{\text{direct}} + p_{\text{reflected}} = \frac{q}{a}e^{jka} + R\frac{q}{b}e^{jkb}, \tag{21}$$

where q is the sound pressure at 1m from the source, a is the distance the direct sound travels and b the reflected path, $k = \frac{2\pi f}{c}$ is the Helmholtz wave number. The reflection coefficient R is defined as:

$$R = \frac{\frac{Z}{\rho_0 c_0}\cos(\theta) - 1}{\frac{Z}{\rho_0 c_0}\cos(\theta) + 1}, \tag{22}$$

where θ is the refraction angle (Figure 3), and the ground impedance Z is approximated with the Delany-Bazley model [19]:

$$Z = \rho_0 c_0 \left[1 + 9.08\left(10^3\frac{f}{\sigma}\right)^{-0.75} - j11.9\left(10^3\frac{f}{\sigma}\right)^{-0.73}\right]. \tag{23}$$

In Equation 23 above σ stands for the *flow resistivity*, a material property describing the viscous pressure losses of the propagating waves in the medium. In the Figure 4 the ground effect is illustrated in both cases, with finite and infinite ground impedance, i.e. $R \neq 0$ and $R = 1$, respectively.

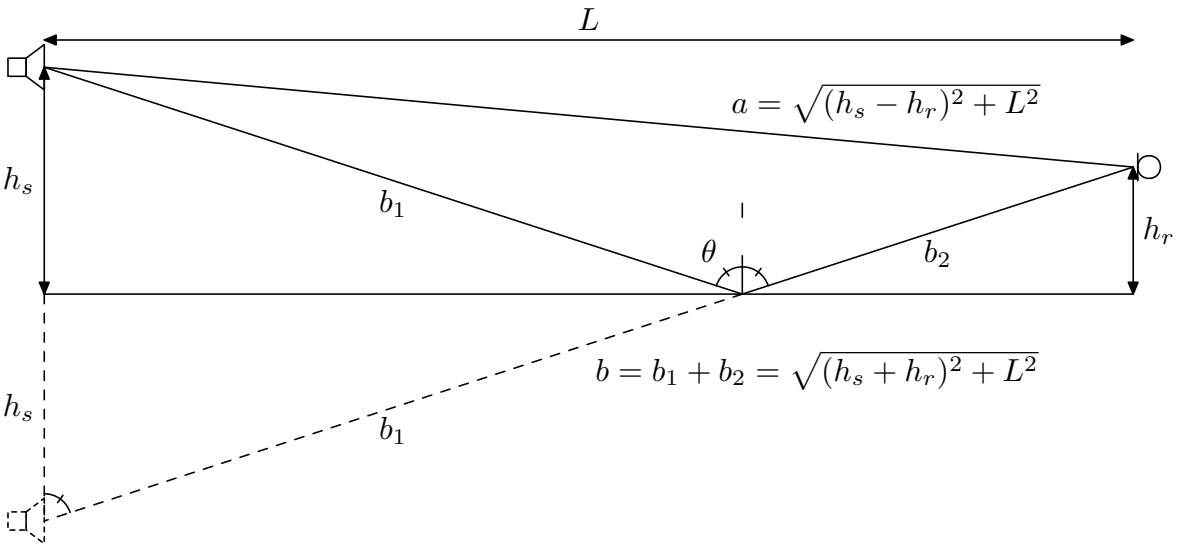

Figure 3: Ground reflection geometry, picture adopted from [20].

From Figure 4 it can be seen that hard ground (infinite impedance) makes deeper dips into the frequency response than porous ground (finite impedance). In other words the reflection from hard ground causes stronger destructive interference at a certain frequency, while the dips caused by porous ground are wider and shifted to lower frequencies. It should be noted that the Delany-Bazley model does not apply well to very low frequencies, and more suitable model have been proposed [21]. In this thesis, calculations are executed using calculation model that uses the Delany-Bazley impedance model.

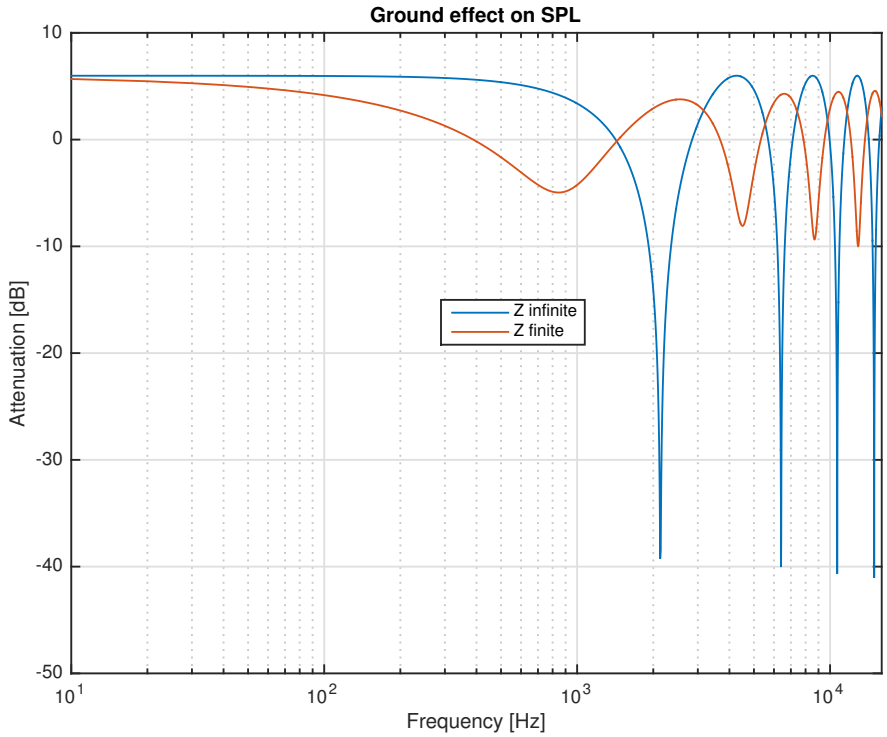

Figure 4: The effect of ground reflections approximated using Delany-Bazley model [19]: finite and infinite ground impedance compared at chosen distance of 9 meters between the source and the receiver. The finite flow resistivity used is $\sigma = 200000 \frac{\mathrm{Ns}}{\mathrm{m}^4}$.

2.2.3 Atmospheric absorption

Atmospheric absorption, or in other words, air absorption is a well known factor attenuating the propagation of sound. It is defined and approximated in standard ISO 9613-1:1993 [3]. The amount of attenuation depends on distance and several ambient conditions like temperature, humidity and pressure. These variables are taken into account in the standard and the atmospheric absorption coefficients as function of frequency and distance are obtained. Frequency dependence for different distances are illustrated in Figure 5.

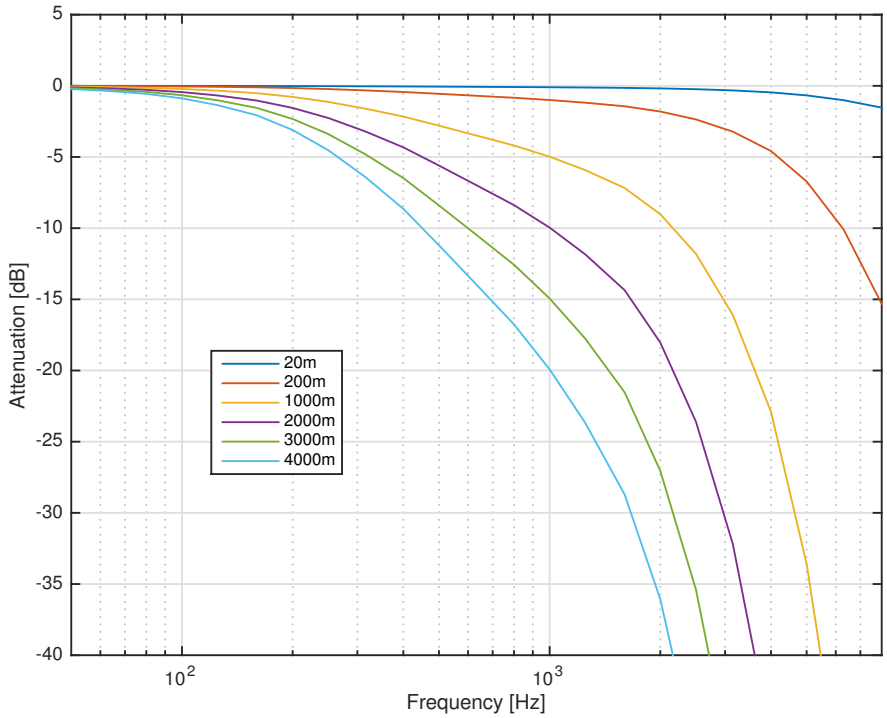

Figure 5: Air absorption for different frequencies at various distances according to ISO 9613-1:2003. Atmospheric conditions used were 20°C temperature and 70% humidity.

As can be seen, at longer distances the absorption of higher frequencies is significant, but for lower frequencies (<100Hz) it is almost negligible.

2.2.4 Turbulent scattering

Turbulent wind occurs usually at ground level, where it results from the changing temperature and wind conditions close to the ground surface. It has an major effect on the sound propagation causing phase and amplitude changes in the sound waves that scatter and merge again after traveling different path lengths. The strength of this effect may vary a lot depending on the surrounding conditions. Generally the amount of turbulence grows as the atmosphere's instability increases. [22]

2.2.5 The effect of weather conditions and the sound speed gradient

Phenomenon where the speed of the sound wave changes is called refraction. It causes a change in the direction of the sound, and may bend the sound waves over obstacles. It can also create *acoustic shadow zones* where the sound waves do not reach as they bend upwards. Sound bends in the medium towards the layer of air with a smaller speed of sound. Assuming a linear height dependence the propagation path of sound waves resemble circular curves. The *sound speed gradient* is the quantity describing the change in speed of sound with altitude. A negative gradient bends the sound waves upwards (more attenuating propagation conditions) and a positive gradient downwards (less attenuating propagation conditions), as illustrated in Figure 7. [2, 22]

Wind speed gradient

The wind gradient describes the increment in wind speed as a function of height. In other words, the wind speed increases in relation to the height above the sea level, and this has a major effect on the speed of sound and sound propagation. For sound propagation, the wind speed component, i.e. the vector between the source and the receiver, can be seen as the factor with most influence [2]. In upwind or sidewind conditions the attenuation can be over 20dB depending on the wind speed and the source-receiver distance, while under downwind conditions the sound level can increase by some decibels.[23]

Temperature gradient

A positive or negative temperature gradient describes how the temperature changes as a function of height. The gradient is positive when the temperature increases upwards, and negative when it decreases, respectively.

On a clear and sunny day the ground warms up and radiates heat, so the layer of air above the ground gets warmer. This results in the temperature decreasing as function of height. On a clear night the heat radiates into skies and the temperature increases upwards. The latter condition is also called *inversion*. If it is cloudy and rainy (or foggy), the temperature stays approximately constant with height. Late studies [24] have also shown that the positive temperature gradient occurs most likely during autumn and winter time.

In addition, there is a surface layer with constant temperature, usually height of the vegetation. These conditions are illustrated in the Figure 6. [2, 22]

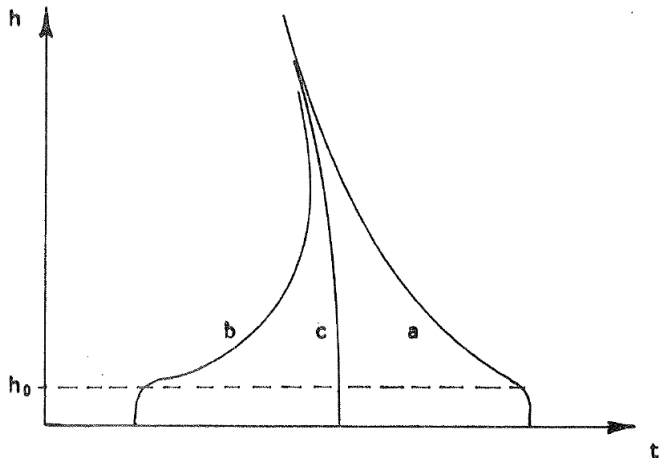

Figure 6: An illustration of the change in temperature as a function of height. h_0 determines the height of the surface layer of air that has a constant temperature. The curves illustrate the different conditions mentioned above: a is for a clear sunny day, b is for a clear night or inversion, and c is for cloudy or rainy conditions. Picture taken from [22].

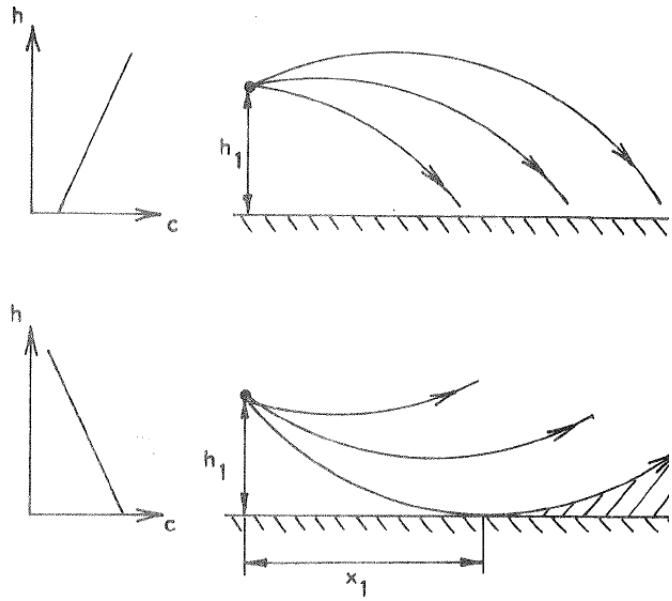

Figure 7: An illustration of the change in the speed of sound with altitude, and its influences on sound propagation. In the upper figure, the speed of sound c increases as a function of height h. This occurs usually under downwind conditions or during inversion and is a favorable condition for sound propagation. Below the opposite case is presented. Note the *acoustic shadow zone* that is illustrated after distance x_1. This results when sound waves bend upwards and do not reach the area at all. Picture taken from [22].

2.2.6 Diffraction

Diffraction is a special case of reflection. It occurs when sound waves encounter an obstacle, or when the waves pass through a narrow opening. As the direct path is blocked, waves bend around the obstacle and spread out. In environmental sound propagation this phenomenon is in most cases more important than the transmission through an obstacle. [4]

Outdoors the obstacle is usually a barrier or a hill. If R_s is the distance from the source to the top of the barrier, R_r is the distance from the top to the receiver and R is the direct path from the source to the receiver, the diffraction at a certain frequency depends on the Fresnel number [4]:

$$N = \frac{2}{\lambda}(R_\mathrm{s} + R_\mathrm{r} + R), \tag{24}$$

where λ is the wavelength of the wave. In order to utilize this, the Harmonoise Engineering Model [25] provides the approximation for the diffraction attenuation (A_diff) for different Fresnel numbers. This is illustrated in Figure 8.

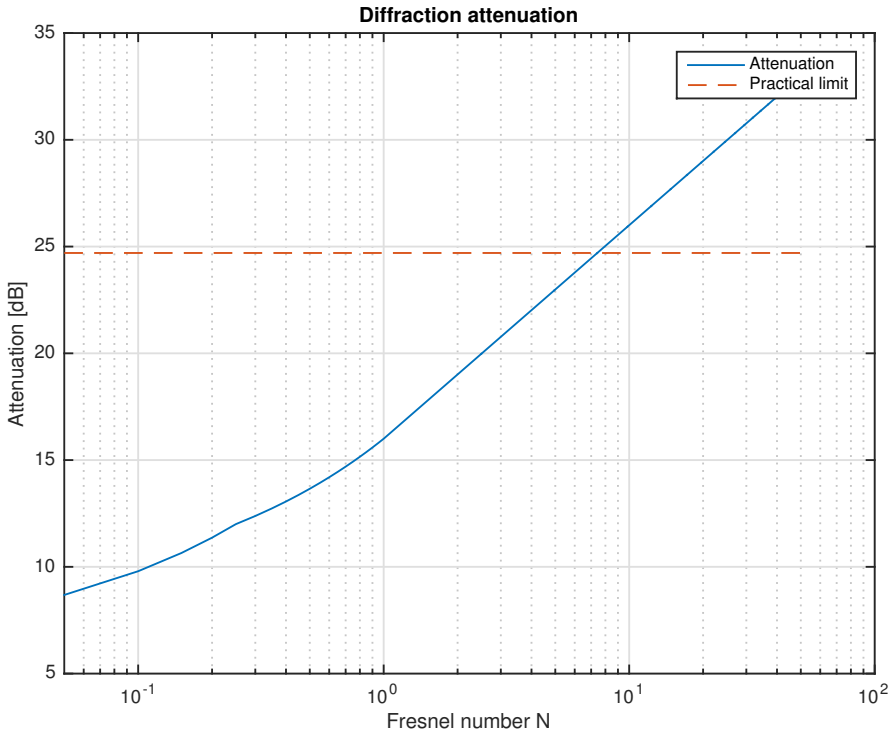

Figure 8: Diffraction attenuation A_diff for different Fresnel numbers calculated according to Harmonoise Model [25]. The practical limit for attenuation is illustrated with dashed red line.

In practice, high Fresnel numbers are hard to achieve when the distances between the source and the receiver are substantial and the frequencies are low. In this case, the application of diffraction for noise abatement is limited, as it would require

impractically large barriers. According to [4], the practical limit for attenuation is just below 25dB.

2.3 Noise generated by heavy weapons and explosions

2.3.1 Sound and vibration formation

Explosions generate high amounts of energy in a short time. In the surrounding environment this causes impulsive noise and vibrations. A sound field does not form immediately, as the detonation creates a rapidly expanding spherical pressure wave that expands non-linearly at multiple times the speed of sound. This *shock wave* is often approximated using Friedlander waveform (Figure 9). It can peak up to a multiple of the static air pressure close to the source, but as the wave expands rapidly, the pressure change rate decreases as the volume of the sphere increases. As a result, the speed of the wave decreases to the level of the sound speed. The linear sound wave has formed, and it starts to propagate and attenuate with distance in a linear way. [26]

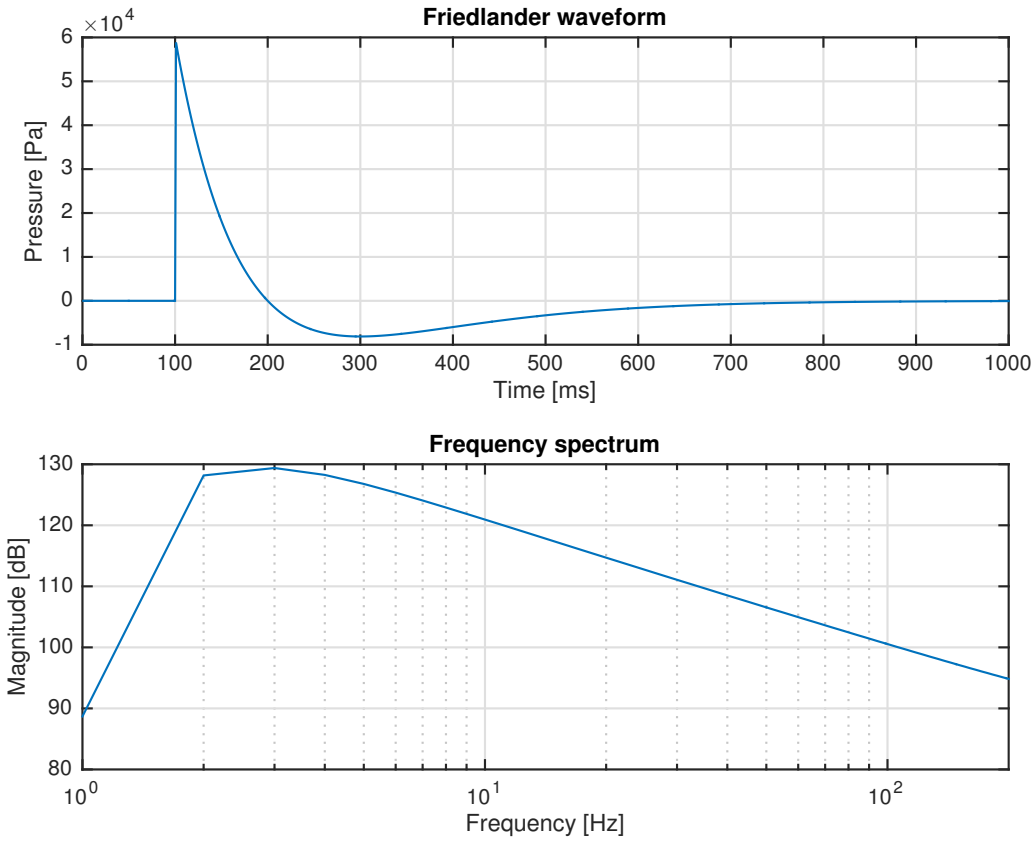

Figure 9: The Friedlander waveform and its frequency spectrum, with decay time of 100ms and 60kPa peak pressure. As can be seen from the spectrum, the frequency content of this theoretical blast is mostly in the infrasound range.

The resulting sound wave has a significant amount of energy at very low frequencies (as can be seen in Figure 9). In order to exceed the threshold of human hearing at low frequencies, a relatively high sound pressure level is needed when compared to higher frequencies. In addition, the sound wave can also cause vibrations in the ground and especially in the building structures. Inside, this is often perceived as audible secondary noise from vibrating surfaces (e.g. floor and windows). [27, 28]

An explosion generates also seismic vibrations that propagate to the receiver through the ground surface with longitudinal and transverse motions. The wave in the ground surface is called *Rayleigh waves*. Studies have shown that if the ground wave occurs at same frequencies that are dominant in the sound wave, the vibrations from ground to structures can be over 100 times greater than in an average situation [28]. However, ground waves attenuate significantly faster in soil compared to the air pressure waves, in the case of open air explosions on ground surface. So, at longer distances the vibrations induced by the airborne pressure wave are dominant at the receiver, as demonstrated in [27].

3 Measurements

The measurements for this work were conducted in Räjähdekeskus's demolition center in Ähtäri. The purpose of the measurements was to gather data from environmental noise levels caused by the detonations of explosive materials and compare the results with measured meteorological conditions measured onsite. The distance between the blast site and the measurement point was approximately 4050 meters, and the direction was about 329 degrees from the north (zero degree reference point). Directions (e.g. wind direction) and locations presented later in this thesis are all represented as degrees in reference to the north with the blast site in the center point. A map of the blast site is presented in Appendix A1.

3.1 Noise measurement equipment and set-up

Equipment

- B&K 2250 Sound Level Meter - Type 2250 [29]
- B&K Sound Calibrator - Type 4231 [30]
- B&K Half-inch free-field microphone, 6.3 Hz to 20 kHz, prepolarized - Type 4189 [31]
- B&K Outdoor microphone kit - UA-1404 [32]
- 2x10m Extension cable
- Manfrotto Tripod

Measurement setup

The sound level meter was placed in a B&K protection case, inside an onsite backup generator container, and powered by line current. The microphone was placed outside using two 10 meter extension cables, and standing on a tripod. The microphone position was selected to avoid sound reflections from the surroundings (container, the forest etc.). Unfortunately, the measurement location is relatively close to a road. The road does not have high traffic, but occasional heavy truck passbys are expected. Also, a generator is located at the site, causing noise that is expected to be found in the measurement results.

The sound level meter was set up to measure 8 hour intervals every day from Monday to Friday, starting from 8 in the morning. Sound recording (16bit Waveform Audio File Format file [33] with f_s=48kHz sampling rate) was triggered to record sounds when $L_{\mathrm{CFmax}} \geq$80dB (rising envelope), and to stop recording when the level is below 70dB. It had a buffer recording 8 seconds before the initial limit is exceeded and 10 seconds after the latter limit is reached.

3.2 Meteorological station

In order to gather weather data a meteorological station was set up in the site. There is a 40 meters tall mast (see Appendix A1, point number 2) with four temperature sensors, three winds sensors, and a humidity sensor. These are installed at different heights starting from ground:

- **2 meters:** Vaisala HMP155 Humidity and Temperature Probe [34] covered with Vaisala DTR13 Radiation Shield [35]
- **10 meters:** Vaisala DTS12A Temperature Sensor [36], Vaisala WAA252 Heated Anemometer [37]
- **20 meters:** Vaisala DTS12A Temperature Sensor [36], Vaisala WMT700 WINDCAP Ultrasonic Wind Sensor [38]
- **40 meters:** Vaisala DTS12A Temperature Sensor [36], Vaisala WAA252 Heated Anemometer [37]

At the height of two meters only the humidity and temperature are measured, and at 10 meters the temperature and wind speed. At 20 meters also the direction of wind is measured among the wind speed and the temperature. At 40 meters only the wind speed and the temperature are measured. Data from the sensors is captured using a Vaisala Automatic Weather Station AWS310 [39] that is capable of storing and distributing the data for further processing or monitoring. An illustration of the system is presented in Appendix B1.

Sensor accuracy

The accuracy of the sensors is presented in the Table 5. Accuracy of the wind speed sensors described in [37, 38] is decent as the gusts of wind cause stronger variation in wind speed (and direction) than the sensor's error can cause, this can be observed e.g. from Figure 22 presented later.

The temperature sensors [34, 36] have more tendency to produce error. As can be seen from the Table 5, the HMP155 can cause ±0.334°C error in 20°C temperature. As the measurements for this work were conducted mostly in summertime, these temperatures are possible. This can cause error when calculating the temperature gradient (celsius per kilometer) between two sensors, for example between 2...40 meters the error could be:

$$T_{\text{grad}} = \pm\frac{0.334°\text{C}}{38\text{m}} * 1000 = \pm 8.8\frac{°\text{C}}{\text{km}}. \tag{25}$$

Due to this and the fact that the first sensor is close to ground and the vegetation level (the constant temperature level), the temperature values used in this thesis will be taken from the higher sensors. To minimize the possible error, that can be ±0.2°C between two sensors, the distance between sensors should be chosen as large as possible. That is, for 10...40 meters:

$$T_{\text{grad}} = \pm\frac{0.2°\text{C}}{30\text{m}} * 1000 = \pm 6.7\frac{°\text{C}}{\text{km}}. \tag{26}$$

The calculated possible error may be significant under still weather conditions when the temperature gradient is close to positive or during the inversion. This error is not remarkable under normal conditions (negative temperature gradient) that are most likely to be expected for daytime conditions.

Table 5: Weather station sensor accuracy according to [34, 36, 37, 38].

Sensor	**Accuracy**
HMP155 (Humidity)	±(1.0+0.008 x reading)%RH at -20...+40°C
HMP155 (Temperature)	±(0.226-0.028 x reading)°C at -80...+20°C
DTS12 (Temperature)	±0.1°C
WAA252 (Wind speed)	$\pm 0.17\frac{\text{m}}{\text{s}}$
WMT700 (Wind speed)	$\pm 0.1\frac{\text{m}}{\text{s}}$ or 2%, whichever is greater
WMT700 (Wind direction)	±2°

4 Methodology

4.1 General noise measurements for heavy weapons and explosions

In order to evaluate and assess the annoyance and harmfulness of explosion generated noise, measurements are needed. The measurements have been performed for this study according to four main references: Ympäristömelun mittaamisohje [40], Ampumaratamelun mittausohje [41], Ympäristömelun arviointi ja torjunta-opas [42] and the standard ISO 1996-(1-3):2003 [43]. The requirements for the used sound level meter are given in [15] as follows:

Properties of sound level meter

- A- and C-weighting filters (IEC class 1)
- Peak time constant
- Hold / maximum
- Max. peak at least 140dB
- Integration circuit for weighted exposure levels $L_{\mathrm{A/CE}}$ and time interval
- Octave band filters 16...8000Hz

Quantities to be measured

- Peak level, L_{Cpeak}
- Sound exposure levels L_{CE} and L_{AE}
- Equivalent noise level, L_{Aeq}
- Octave band analysis

The noise measurements for heavy weapons and explosions consist of two phases. The first phase is called control phase, where only the noise peaks L_{Cpeak} is measured. If L_{Cpeak} exceeds 115dB the second phase (full measurements) is needed. In the measurement phase, C-weighted peak and sound exposure levels (L_{Cpeak}, L_{CE}) are measured together with A-weighted equivalent level and sound exposure level (L_{Aeq}, L_{AE}). Octave analysis is also conducted. The measurements are put together in a document that holds all the information about the equipment, calibration, measurement results and surrounding conditions.

If surrounding conditions do not meet the requirements stated in [40], it shall be mentioned in the document. This may be caused by the weather impact on the sound propagation, as weather is the biggest factor causing dispersion in the measurement results. The weather information during measurements is usually verified on site or from a weather observation, noting the air temperature, humidity, air pressure, wind speed and direction and cloudiness. In this thesis, this weather data comes from the onsite meteorological station.

4.2 Noise propagation prediction

It is not always reasonable or possible to conduct long-term measurements in order to find out how noise propagates in the environment. Models for predicting noise propagation have been developed for this reason; they represent long-term averages and wanted conditions while measurements contain large variations. Originally, these models were developed to be used in manual calculations and predictions, but as technology has developed further, propagation models have also been compiled into computer programs. This section introduces the most important current noise prediction models, and also presents how to predict the influence of weather on the sound propagation in order to make a hypothesis for one of the research questions of this thesis.

4.2.1 Noise modeling

General Prediction Method

The common method used in the Nordic countries is the General Prediction Method (GPM) [44] published by the Danish Acoustical Laboratory and released in 1982. Its original purpose was to be used for predicting noise immissions in areas close to industrial plants, but it has been successfully applied to the prediction of noise in many other sectors as well. The prediction model is based on empirical measurements and calculations, and it was designed to work for distances less than 1000m in the 63...8000Hz frequency range.

The calculation model was not originally developed to be computerized, and it makes some assumptions about surrounding conditions. In the calculations, a neutral temperature gradient (no height dependence) and moderate downwind away from the source are presumed. As mentioned earlier, the weather conditions have a major effect on sound propagation so in many cases the model may yield false predictions. Another limitation would be that the ground reflection does not take frequency into account for different types of soil. The ground is seen as hard or soft ground. This is also an important factor as different frequencies behave divergently when propagating.

Nord 2000 model

As mentioned, the GPM had some important parameters left out in the calculations and it was not optimized for computers. The Nord 2000 method [45] was presented in the beginning of the 21st century. This model was intended to be utilized in computer software and this novel prediction model had taken into account many of the parameters missing from the older model. It is far more complex than GPM and designed originally for general environmental purposes and not only for industrial noise abatement. Table 6 shows the key differences between the old and new model.

The new model has adjustable wind speed and temperature gradient in order to predict the sound propagation in different weather conditions. Turbulent scattering is also included. These phenomena induce, as mentioned earlier, sound waves to

bend over obstacles or into shadow zones behind them. According to [46] the possible weather parameters in Nord 2000 are:

- Windspeed
- Standard deviation of wind speed
- Wind direction
- Temperature gradient
- Standard deviation of the temperature gradient
- Turbulence strength parameter for wind
- Turbulence strength parameter for temperature
- Roughness length

Discontinuities in screening, or barriers, are also taken into account. In the old GPM, double screening occurs if the distance between barriers is 0.2-0.3 times the distance between the source and the receiver, while in Nord 2000 these barriers are seen as single barriers. Also complex terrain profiles and the ground's specific acoustic impendance are taken into account. As the model is computerized, the calculation results are less user dependent and the software defines many factors that have been up to the users' knowledge earlier. [46]

Comparative studies conducted in [46] show remarkable differences in different weather conditions between the two above mentioned models. For downwind the results are within a few dB, but on upwind the GPM gives 6-7dB higher results (at 200m) than Nord 2000, and at 300m the difference is over 10dB. The comparison also shows that the GPM overestimates the noise level behind screens, especially under upwind conditions. Also the ground reflections alongside the barriers, taken into account in Nord 2000, cause differences between noise levels. Note, that GPM is not designed to be accurate under upwind as it has no changeable weather conditions, these comparisons only demonstrate the differences caused by the parameters in these two models.

Noise modeling software

DataKustik CadnaA (Computer Aided Noise Abatement) software [47], used in this thesis, is a state-of-the-art preditcion software for modeling and assessing noise.

It has over 30 built-in calculation models for predicting industrial, roadway, railway and aircraft noise with 3D visualization possibilities and graphical user interface. It can also be extended for assessing and presenting air pollutant distribution. It is designed to communicate with Windows applications like word processors, spreadsheet calculators, CAD software (Computer-aided drafting) and GIS-databases (Geographic Information System). The terrain model used in this thesis is imported to CadnaA from GIS-database provided by National Land Survey of Finland (Maanmittauslaitos). The used terrain model is illustrated in Appendix C1.

Table 6: Differences between the General Prediction Method and Nord2000.

Property	**GPM**	**Nord2000**
Divergence	Yes	Yes
Air absorption	Yes	Yes
Reflections (obstacles)	Yes	Yes
Scattering	No	Yes
Barriers	Yes	Yes (complex)
Vegetation	Yes	Yes
Complex terrain	No	Yes
Specific acoustic impedance of the terrain	No	Yes
Turbulent scattering	No	Yes
Wind Speed	Constant	Adjustable
Temperature gradient	No	Adjustable
Designed to be computerized	No	Yes

The sound source model

In order to predict the immission at the receiver, an approximation for the (energy) emission of the sound source is needed. In this thesis the source is modeled applying the Weber spectrum, adopted in the ISO 17201-2 standard [48], as a sound source. The model takes the amount of explosive compound in grams as input and calculates an approximation for the weighted total energy levels and also the corresponding octave spectrum (to be used in the prediction software later).

According to this approximation, the charge size affects the highest peak frequency. For charges over about 50kg the peak frequencies are at very low frequencies, i.e. at *infrasound* range, that is below 20Hz.

In the Figure 10 the calculated total energy emissions (L_{JZ}) for different amounts of TNT are presented. It can be seen, that the difference between 10kg and 100kg charges is about 10dB, between 40kg and 100kg under 5dB, and the range 100...250kg results also under 5dB. This means, at least in theory, that the charge does not have a major effect on the total sound pressure level in the 40...250kg range.

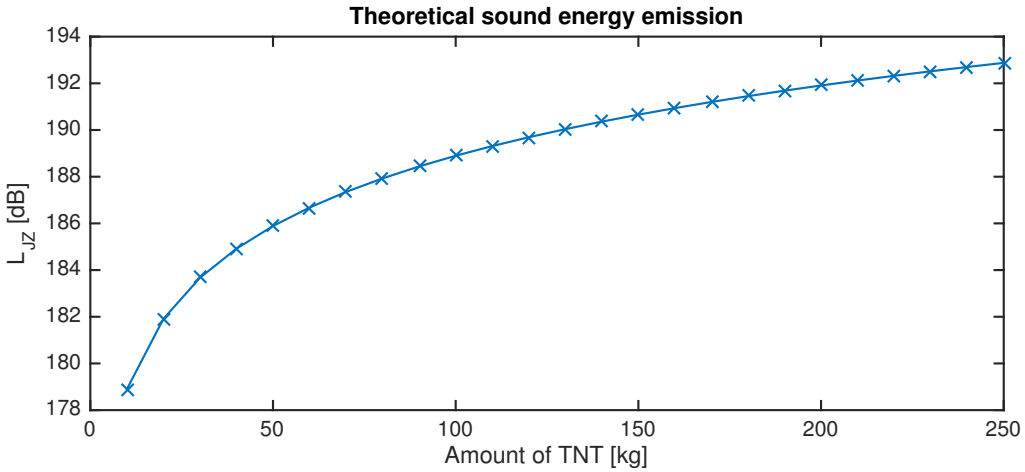

Figure 10: Theoretical sound energy emission (linear total) for different charges of TNT, calculated using the Weber spectrum. The dependence between the charge size and energy emission L_{JZ} resembles logarithmic behavior.

It is noteworthy to mention that the Weber spectrum was calculated for the frequency range 4Hz...8000Hz, while CadnaA takes the emission input as an octave spectrum only in the range 31.5Hz...8000Hz. Hence, the sound energy in the lowest octave bands was summed into the 31.5Hz band for predictions and in the calculations 4...16 Hz octaves propagation was assumed the same as for 31,5 Hz octave.

4.2.2 Predicting the impact of the meteorological conditions on noise levels

As mentioned, changes in the atmosphere have a large effect on sound propagation. Phenomena like wind and temperature gradients or turbulence are the result of many factors. For instance, solar radiation heats the ground and warm air rises upwards

(*thermal column*). Clearly, there is no trivial way to assess all the factors and evaluate their effect on each other. So to simplify, the surrounding meteorological conditions can be classified into *stability classes* or *weather classes* in order to estimate the sound propagation [2, 49].

The principle for classifying the surrounding meteorological conditions is to divide them into three classes: *unstable*, *neutral* and *stable*, but in practice, the classes are divided into six Pasquill classes (A-F) [2]. Unstable conditions (classes A and B) occur when solar radiation is strong causing a thermal column which results in turbulence. The atmosphere is said to be stable (classes D and F) when radiation from the sun is weak and turbulence due a to thermal column does not occur. Neutral atmospheric conditions (classes C and D) are between the two aforementioned. Such conditions occur usually under windy conditions, combined with low radiation from the sun.

In Table 7 the Pasquill classes are presented in respect to the wind speed and solar radiation. In addition to the conditions listed in the table, the weather class is set to be D for all wind speeds about one hour before sunset and one hour after sunrise. It should be noted, that the neutral weather class must not be confused with *acoustically neutral* conditions as wind has an remarkable effect on the sound propagation. Also, it is worth noting that a large wind speed and temperature gradients cannot coexist, as they are not independent of each other. [2, 49, 50]

Table 7: Pasquill weather classes for day and night according to [2].

Wind speed$[\frac{m}{s}]$	**Solar radiation (Day)**$[\frac{mW}{cm^2}]$				**Cloud cover (Night)**		
	≥ 60	30-60	≤ 30	Overcast	0-4	4-7	8 [octas]
$\leq$1.5	A	A-B	B	C	F	F	D
2.0-2.5	A-B	B	C	C	F	E	D
3.0-4.5	B	B-C	C	C	E	D	D
5.0-6.0	C	C-D	D	D	D	D	D
$\geq$6.0	D	D	D	D	D	D	D

It is also possible to describe the wind speed categories (W) and also the temperature gradient (TG) using qualitative representations. The qualitative descriptions are presented in Table 8. [2, 50]

From the above mentioned qualitative wind and temperature values is logical to proceed to sound propagation. Studies [2, 50] have shown that qualitative attenuation or enhancement of sound can be estimated for different weather conditions. It is typical that in practice there are more attenuating conditions than enhancing, and the attenuation is usually much stronger (5-20dB) than the possible enhancement (1-5dB) [2]. The qualitative estimates for the sound propagation are presented in the Table 9, based on the above mentioned qualitative wind categories and temperature gradients. Even though the attenuation rate changes in a large scale, it is safe to say that there are such weather conditions where the attenuation between the source and the receiver is most probably at its largest, and so the noise propagation can be estimated.

Table 8: Qualitative representations for wind categories and temperature gradients [2, 50].

W1	Strong wind (>3-5$\frac{m}{s}$) from receiver to source
W2	Moderate wind (≈1-3$\frac{m}{s}$) from receiver to source, or strong wind at 45°
W3	No wind or any cross wind
W4	Moderate wind (≈1-3$\frac{m}{s}$) from source to receiver, or strong wind at 45°
W5	Strong wind (>3-5$\frac{m}{s}$) from source to receiver
TG1	Strong negative gradient: daytime with strong radiation (high sun, little cloud cover), dry surface and little wind
TG2	Moderate negative temperature gradient
TG3	Near isothermal: early morning or late afternoon
TG4	Moderate positive: night-time with overcast sky or substantial wind
TG5	Strong positive: night-time with clear sky and little or no wind

Table 9: Qualitative estimates for sound propagation, according to [2]. The largest attenuation is most probably obtained at high wind speeds or strong negative temperature gradients.

	W1	**W2**	**W3**	**W4**	**W5**
TG1	-	Large attenuation	Small attenuation	Small attenuation	-
TG2	Large attenuation	Small attenuation	Small attenuation	Zero meteorological influence	Small enhancement
TG3	Small attenuation	Small attenuation	Zero meteorological influence	Small enhancement	Small enhancement
TG4	Small attenuation	Zero meteorological influence	Small enhancement	Small enhancement	Large enhancement
TG5	-	Small enhancement	Small enhancement	Large enhancement	

4.2.3 Nord 2000 performance test on the effects of weather conditions

As mentioned, the Nord2000 method is able to take different weather conditions like wind and temperature into account. Calculations were performed using DataKustik CadnaA software [47] in a simple way, calculating the sound exposure levels from source to receiver. A flat reflecting ground without any terrain model was used at this point.

The application of a 3D terrain model was found to be too heavy to be calculated in reasonable time when using grid plotting. This may be due to the fact that the CadnaA software is not optimized to use more than one computer core for Nord 2000 calculations. For this reason, CadnaA calculations presented later in this thesis have been calculated in the same way (source to receiver), but using the created terrain model for the Ähtäri blast site and its surrounding.

The meteorological conditions were chosen based on Table 8. Wind speed was chosen to be 0, 1, 3 or $5\frac{m}{s}$, and the temperature gradient -20, -8, 0, 8 or 20 degrees Celsius per kilometer. The other parameters like humidity and temperature were kept constant. The source energy emission was approximated using the Weber spectrum for an explosion of 108kg of TNT. To be noted, as Cadna takes spectrum as an input starting only from the 31.5Hz octave band, the sound energy at the lower octave bands (4...16Hz) is summed into this band. The calculation points (receivers) were evenly spaced out on a line parallel to the wind direction, with a spacing of about 2.5km upwind and downwind from the source.

The results of the prediction were similar to the Table 9. The results for total exposure levels L_{AE} are presented in Figure 11 and in Figure 12 the L_{CE}. The distance to the source is 5km, as it is close to the distance of the actual measurement point introduced later. The center of the result table illustrates the zero conditions with no wind or temperature gradient. This zero condition does not represent neutral conditions in term of sound propagation, but it is used as a reference point in order to find out how different parameters affect the results.

The calculated attenuations seem to be remarkably higher than the amplifications, as stated previously in theory. Also, it can be seen that wind has a dominant effect when compared to the temperature gradient. The only exception is with a high positive gradient and wind, when less attenuation is achieved compared to the other cases. As stated before, a strong wind and a strong temperature gradient cannot coexist, so these conditions are left out from the calculations.

Nord2000: LAE 5km	W1 -5m/s	W2 -3m/s	W3 -1m/s	W4 0m/s	W5 1m/s	W6 3m/s	W7 5m/s
TG1 -20 celsius/km		52.1	58.5	67.6	77.2	77.4	
TG2 -8 celsius/km	48.6	52.4	59.1	71.5	77.2	77.5	77.8
TG3 0 celsius/km	48.7	52.6	59.6	77	77.3	77.8	78.2
TG4 8 celsius/km	48.8	52.8	60.1	77.1	77.6	78.1	78.5
TG5 20 celsius/km		61.6	66.6	77.6	78.1	78.6	

Nord2000: LAE 5km	W1 -5m/s	W2 -3m/s	W3 -1m/s	W4 0m/s	W5 1m/s	W6 3m/s	W7 5m/s
TG1 -20 celsius/km		-24.9	-18.5	-9.4	0.2	0.4	
TG2 -8 celsius/km	-28.4	-24.6	-17.9	-5.5	0.2	0.5	0.8
TG3 0 celsius/km	-28.3	-24.4	-17.4	0	0.3	0.8	1.2
TG4 8 celsius/km	-28.2	-24.2	-16.9	0.1	0.6	1.1	1.5
TG5 20 celsius/km		-15.4	-10.4	0.6	1.1	1.6	

Figure 11: Calculated Nord2000 sound exposure levels L_{AE} for various wind speed and temperature gradient combinations. Upper figure: the sound exposure levels; lower figure: relative attenuations compared to conditions with no wind or temperature gradient.

Nord2000: LCE 5km	W1 -5m/s	W2 -3m/s	W3 -1m/s	W4 0m/s	W5 1m/s	W6 3m/s	W7 5m/s
TG1 -20 celsius/km		91.8	96.6	100.3	101.5	101.5	
TG2 -8 celsius/km	88.4	92	96.9	101	101.5	101.7	101.9
TG3 0 celsius/km	88.6	92.2	97.2	101.3	101.8	102.2	102.4
TG4 8 celsius/km	88.7	92.4	97.4	101.8	102.3	102.6	102.8
TG5 20 celsius/km		94	99	102.4	102.9	103.2	

Nord2000: LCE 5km	W1 -5m/s	W2 -3m/s	W3 -1m/s	W4 0m/s	W5 1m/s	W6 3m/s	W7 5m/s
TG1 -20 celsius/km		-9.5	-4.7	-1	0.2	0.2	
TG2 -8 celsius/km	-12.9	-9.3	-4.4	-0.3	0.2	0.4	0.6
TG3 0 celsius/km	-12.7	-9.1	-4.1	0	0.5	0.9	1.1
TG4 8 celsius/km	-12.6	-8.9	-3.9	0.5	1	1.3	1.5
TG5 20 celsius/km		-7.3	-2.3	1.1	1.6	1.9	

Figure 12: Calculated Nord2000 sound exposure levels L_{CE} for various wind speed and temperature gradient combinations. Upper figure: the sound exposure levels; lower figure: relative attenuations compared to conditions with no wind or temperature gradient.

4.3 Data acquisition and processing

4.3.1 Audio data and processing

In order to assess the noise from blasts, the recorded sound pressure signals were analyzed separately. The sound level meter used is Brüel & Kjaer Type 2250 [29], which is able to calculate the required parameters and level quantities. However, in this thesis the chosen approach was to develop Matlab tools for the wave file analysis. The explosion signal is recorded as a 16bit Waveform Audio File Format file (.wav, [33]) at 48kHz sampling frequency. Actually, the meter itself uses a 24bit resolution, but this is converted to 16bit when recording to a wave file.

From the wave files, blasts are extracted using a suitable software (Adobe Audition [51]) and then processed using Matlab. The signal processing flowchart is presented in Figure 13.

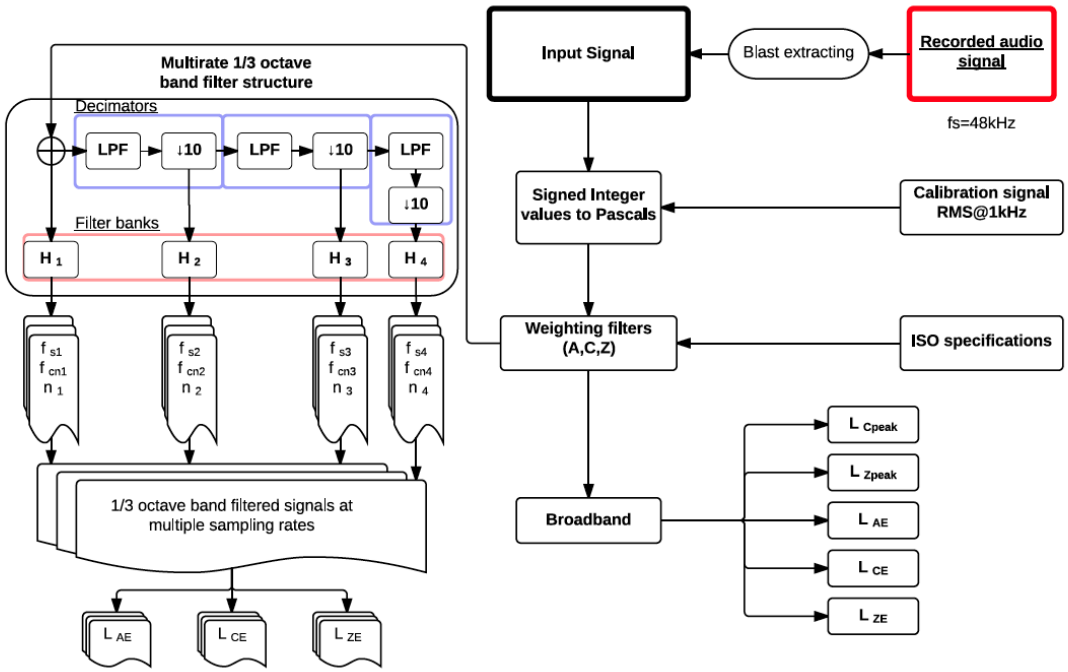

Figure 13: Signal processing flow chart. The decimators are highlighted with light blue and the one third octave filter banks with light red.

Broadband

After blast extraction, the input signal is calibrated using the recorded calibration signal. This means converting the signed integer values of the wave file into sound pressure (Pascals). After this, the frequency weighting filters are applied. The frequency weightings used are the previously mentioned A- and C-weightings, and the non-weighted signal. The weighting is implemented using Christophe Couvreur's Octave Toolbox [52, 53], and the frequency responses of the weighting filters are

found in the Figures 14 and 15. From the weighted signal, the broadband parameters can be calculated using the equations presented in the Section 2.

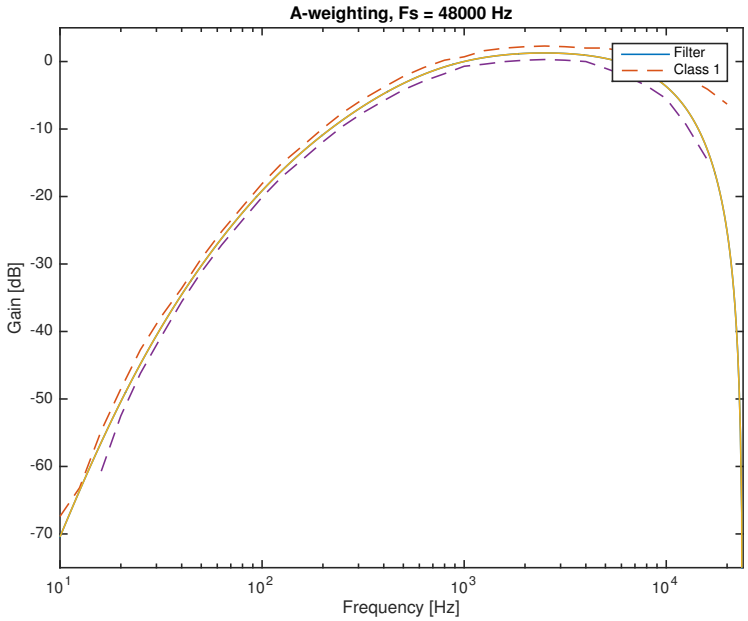

Figure 14: Frequency response of the designed A-weighting filter that fulfills the IEC class 1 [54] requirements.

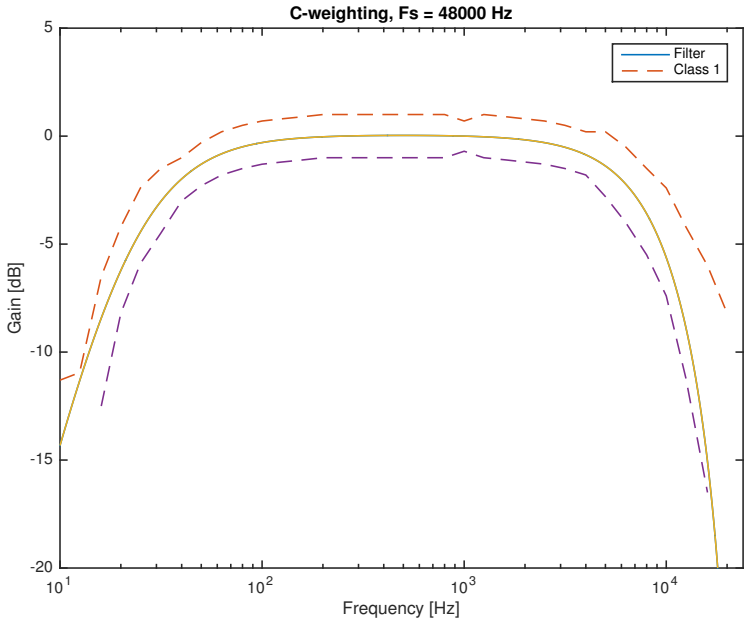

Figure 15: Frequency response of the designed C-weighting filter that fulfills the IEC class 1 [54] requirements.

Spectral analysis in one third octave bands

In order to analyze the third octave band spectrum and parameters, more complex processing is needed. The solution used was to create multi rate filter bank structure, that processes the data in four different sampling rates, and create one third octave band filters that meet the IEC 1260 standard [54].

Matlab's own implementation of fractional octave band filters does not meet the IEC requirements below approximately 100Hz, when the center frequence of the filter is much smaller than the sampling frequency. As the goal was to analyze signals down to the 1Hz band, filter design was needed. The designed filters are 8th order Butterworth filters, using the band cut-off frequencies presented in [7, 1]. An example of the fractional-octave band filter is shown in Figure 16. The figure illustrates the IEC standard limits for the 1Hz third octave band filter, and the plotted filter (sampling frequency 48Hz). The IEC limits in the figure are plotted using the Octave Toolbox [52, 53].

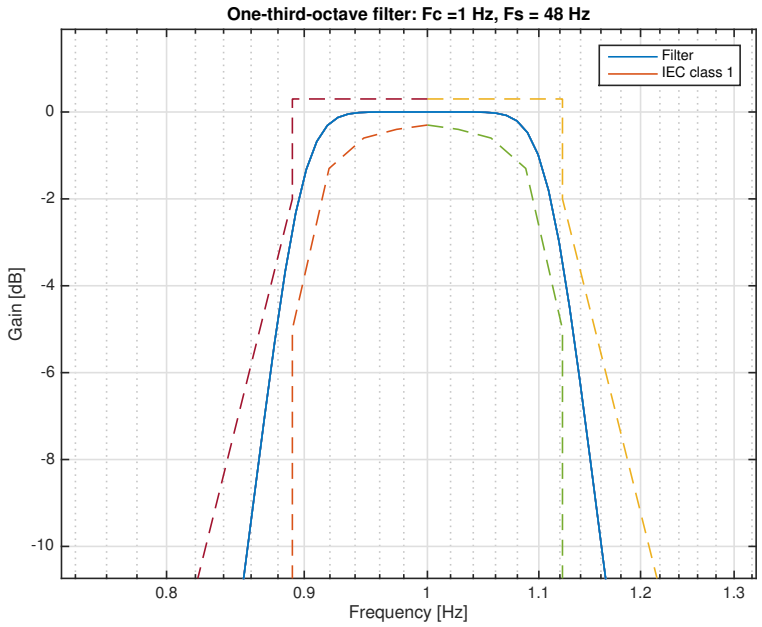

Figure 16: Designed one third octave band filter at 1Hz band. As can be seen, it meets the IEC class 1 requirements [54].

In order to get to the low frequencies, decimation was needed. The starting sampling frequency was 48kHz, and it was decimated three times by 10, giving three new signals with sampling rates 4800Hz, 480Hz and 48Hz. Before downsampling, each signal was low pass filtered in order to avoid aliasing. The anti aliasing filter used was a 500th order finite impulse response filter (FIR) with Hanning window. The cut-off frequencies were chosen below the half of the target sampling frequency.

At low frequencies, the filter's impulse response was found out to be remarkably long (example in Figure 17). This leads to a temporal spreading of energy, which

results in a distorted amplitude spectrum. Testing with a 10 second long multitone signal, containing a sinusoid with amplitude of one at every third octave band, should give an amplitude spectrum with equal amplitudes. However, in the results (Figure 18), some energy loss can be seen at low frequencies. Using a longer test signal, shown in Figure 19, the result was found out to get close to the correct value.

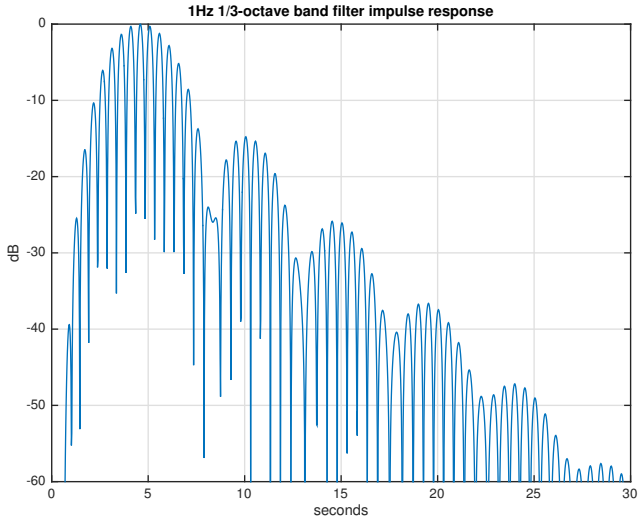

Figure 17: Impulse response of the 1Hz band of one third octave band filter. As can be obtained, the impulse response is remarkably long. This causes temporal spreading of energy that results as distorted amplitude spectrum.

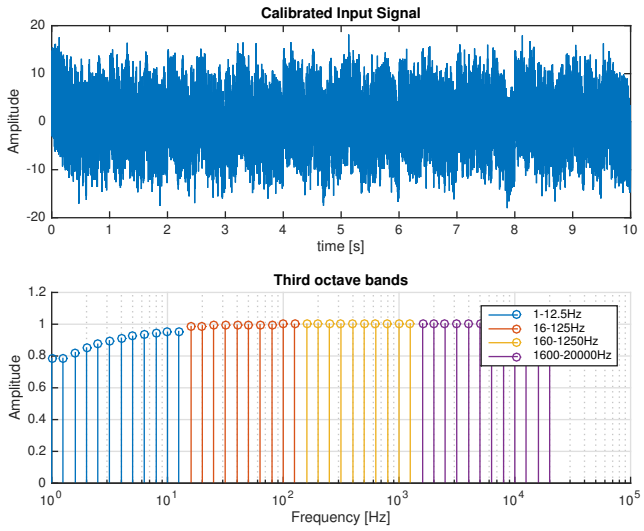

Figure 18: Amplitude spectrum using a 10s multi tone test signal. The energy losses are found at low frequency bands, this is due to the length of the impulse response in comparison with the test signal.

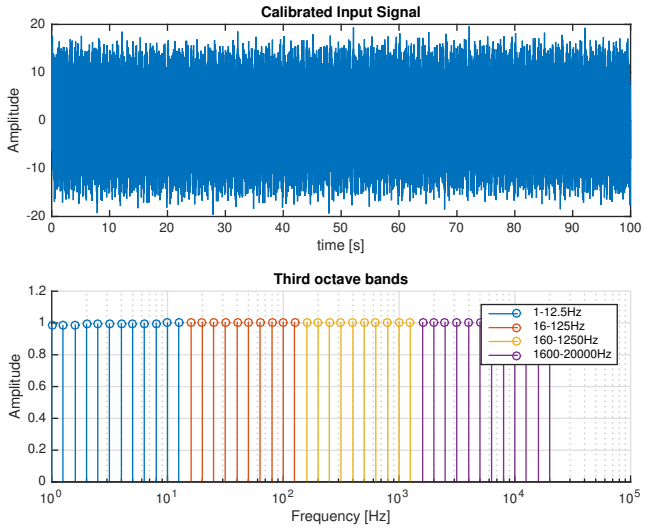

Figure 19: Amplitude spectrum using a 100s multi tone test signal. Note that improved results are obtained with longer test signal when compared with the shorter test signal.

This phenomenon was resolved by zero padding the blast signals to be analyzed. To verify the Matlab filter and calculated parameters the results from Matlab were compared with three other methods. Figure 20 shows the comparison of the following methods: B&K Sound Level Meter's software [29], imc FAMOS [55], the Matlab analysis, and FFT spectral analysis with Spectra Plus Software [57]. The FAMOS was selected to stand as a reference method as its one third octave filtering is stated to fulfill standards IEC 1260, DIN IEC 651, DIN 45652 and DIN EN 61260, that are currently covered in the IEC 61672-1 and IEC 61260-1 standards [8, 56]. The selected parameter to be compared was L_{ZE}, the Z-weighted exposure level. To be noticed: the lowest possible band reached by the B&K and FFT software is 6.3Hz, while FAMOS and Matlab both reach down to 1Hz.

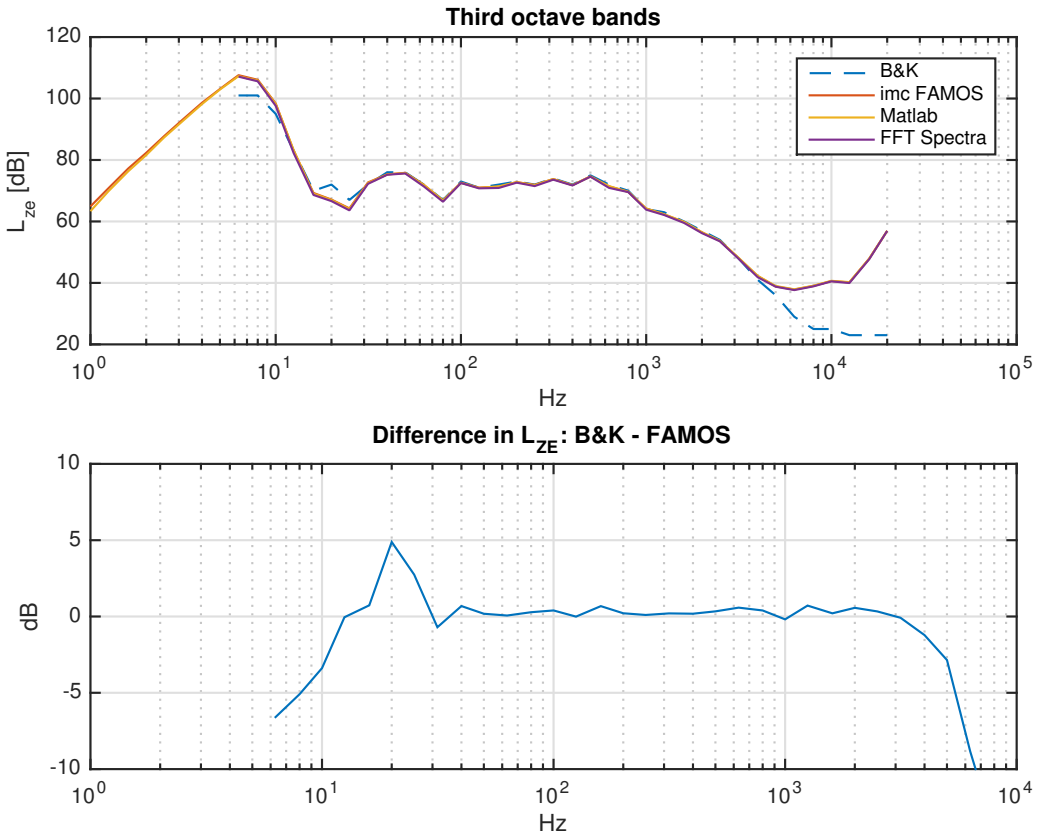

Figure 20: Above, one third octave spectra by Matlab analysis, imc FAMOS, FFT and B&K are plotted. As can be observed, some interesting differences are seen in the B&K plot. Below, the difference between FAMOS and B&K is being plotted in one third octave bands. It can be noticed, that the difference is ±5dB around 6Hz...30Hz

As can be seen, the Matlab analysis, FAMOS and FFT all give similar results. The B&K software has a clear difference (about ±5dB) at bands below 31.5Hz. This can be seen also in the Table 10, where the total exposure levels are presented for bands 6.3Hz...25Hz and 31.5Hz...20kHz. It is also noticeable in Figure 20, that the spectra at higher frequencies differ between the B&K and the other systems. This is due to fact that B&K uses the 24bit hardware resolution, leading to a higher dynamic range compared to the other methods, which use the data from a 16bit wave file in the analysis.

Table 10: Z-weighted total exposure levels calculated from the one third octave spectrum with different software.

Total L_{ZE}	**B&K**	**FAMOS**	**Matlab**	**FFT**
6.3Hz-25Hz	104.5	110.2	109.9	109.7
31.5Hz-20kHz	84.8	84.6	84.6	86.4

The comparison between FAMOS and the developed Matlab analysis (starting from 1Hz) is presented in the Figure 21. As can be seen, the resulting L_{ZE} is approximately the same throughout the band, the biggest difference is -1.6dB at 1Hz and at 2Hz it is already only -0.4dB. As a conclusion, Matlab analysis was found applicable to be used in this work.

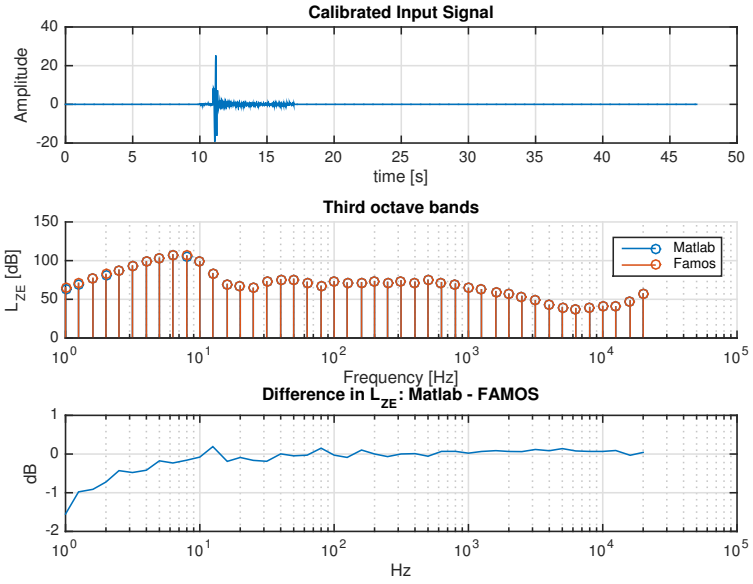

Figure 21: Matlab vs. imc FAMOS, analysis of a recorded blast signal . The the first plot illustrates the calibrated time signal, the second is the one third octave spectrum from Matlab and FAMOS. As can be seen, the differences cannot be seen from this plot and thus the third plot represents subtraction of the mentioned methods at the bands under inspection.

In addition, when comparing Figures 20 and 21 to the theoretical Friedlander waveform in Figure 9, there can be noticed similar shape in the spectrum. The differences are due to the sound propagation discussed earlier, reverberation in the forest and the ground effect. As an example, the ground reflection dips from Figure 4 can be noticed e.g. around the 12.5Hz band.

4.3.2 Meteorological data

The gathered weather data needs no signal processing treatment, and it can be used as it is. Though, in order to utilize the data, some calculation must be done. For example, the temperature gradient is usually reported as temperature change in degrees (Kelvin or Celsius) per kilometer. This can be obtained from the difference between the readings of the temperature sensors at different heights.

The wind speed component v' parallel to the sound propagation path from source to receiver is calculated using the known wind speed v ($\frac{m}{s}$), wind direction β (degrees) and the receiver location at an angle α from the source. Using trigonometry the wind speed component v' can be defined as:

$$v' = -v * \cos(\beta - \alpha), \tag{27}$$

where the minus sign determines the upwind or downwind conditions for the sound propagation depending on the wind direction.

When it comes to analysis, the weather parameter to be utilized with the noise measurement results had to be chosen. The possibilities were a two or ten minutes average (also minimum and maximum), or instant values for each noise event. The chosen parameter was the average of two minutes, as it takes some variation in the conditions into an account, but is not too sensitive for small deviations. A ten minutes average would give slightly different values, but as the intent of this thesis is to find out if the data from the weather station can be used to evaluate current sound propagation conditions, two minutes is justified. The instant values reflected well the changes in the transient conditions, as for example wind speed variations were remarkable within short time intervals.

Figures 22 and 23 illustrate plotted examples of the weather data acquisition system output. In the Figure 22 deviations in the temperature, wind speed and wind direction are presented over time. Earlier mentioned temperature and wind speed gradients are shown in the Figure 23, as the temperature and wind speed change as a function of height.

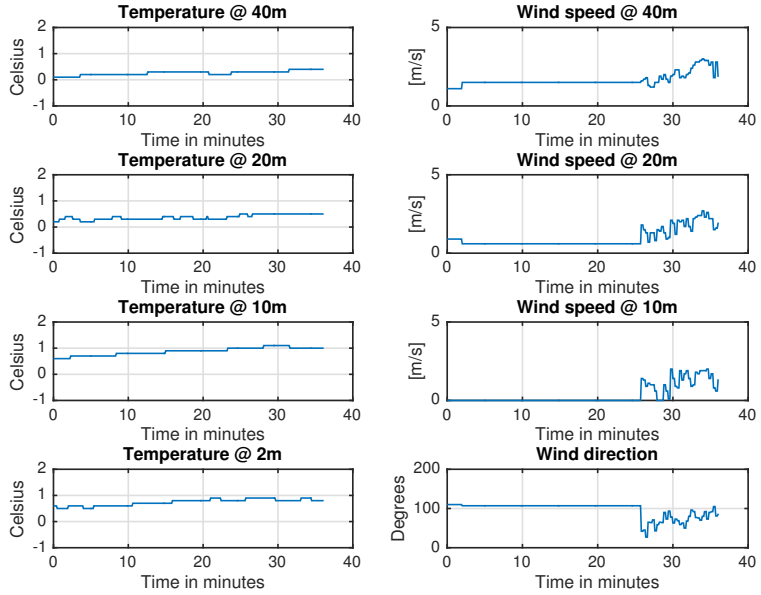

Figure 22: Temperature, wind speed and wind direction deviations over a test period of time. Note that the variation in temperature is modest over time, but the changes in wind speed and direction are more notable.

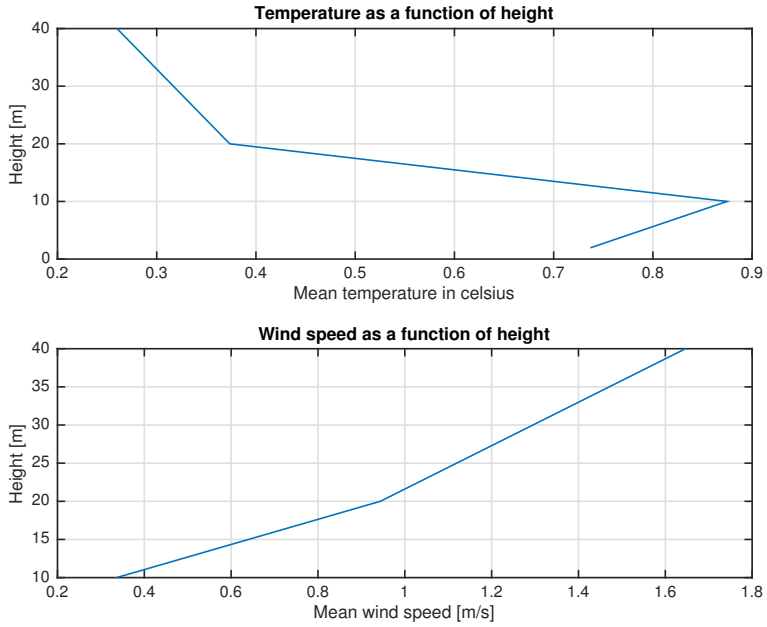

Figure 23: Examples of temperature's and wind speeds's height dependence. The temperature data shows negative temperature gradient, excluding the value from sensor at 2 meters, which is considered here as vegetation level. The wind speed shows almost linear height dependence between the sensors.

5 Results and analysis

In this section the measurement results are presented, analyzed and discussed in comparison with each other and the calculation model. The propagation model used is the Nord 2000 model calculated with the CadnaA software. The weather station gives the parameters for wind and approximated temperature gradient to be used in the modeling, so the conditions are re-created to match the propagation conditions during the measurements. In addition to the audio signal processing in Matlab, some data presented in this section was also processed using Microsoft Excel [58].

Due to a number of unforeseen technical and logistical difficulties that occurred in first half of the measurement period, the data amount obtained from the primary measurement point was relatively small (25 blasts). For this reason, some data from older measurements [26] conducted at the same site was included. In addition, a second sound level meter (01dB Duo [60]) was set-up on site, and some blasts were recorded with it. All these measurements were done according to the guidelines for heavy weapon noise [15], and documented including approximated meteorological conditions. It should be noticed, that the meteorological station was not set up at the time of the old measurements, so the temperature gradient cannot be calculated and taken into account. This has been taken into account in the analysis of the older data.

As the above mentioned extra data was not recorded at the same measurement point as the original, the distances from the measurement positions to the sound source were normalized applying the Equation 20, i.e. assuming a point source. Total number of independent blasts is 44.

5.1 Measurement results

5.1.1 Meteorological conditions during measurements

The measured meteorological conditions during the noise measurements are presented in the Figure 24. These include the wind speed and the calculated temperature gradient. The wind speed varied between $1.65\frac{m}{s}$...$8.5\frac{m}{s}$ and was mostly strong wind (over $4\frac{m}{s}$). The corresponding temperature gradients were between -$30\frac{^{\circ}C}{km}$...-$10\frac{^{\circ}C}{km}$. As can be observed, no occurrence of positive temperature gradient or inversion were measured, unfortunately.

Figure 24 shows that the highest temperature gradients are obtained when the wind speed is highest, but there is also variation even in the same wind conditions. As wind speed increases as function of height, it is logical that the faster moving air is cooler than the air closer to the ground or vegetation level. Note that the wind speeds in the figure are direct readings from the sensor. These values do not portray the component parallel to the receiver direction, nor does not take the direction into account.

Wind speeds and their corresponding wind directions are presented in the Figure 25. It can be seen, that the wind direction at the site was mostly between 150° and 270°.

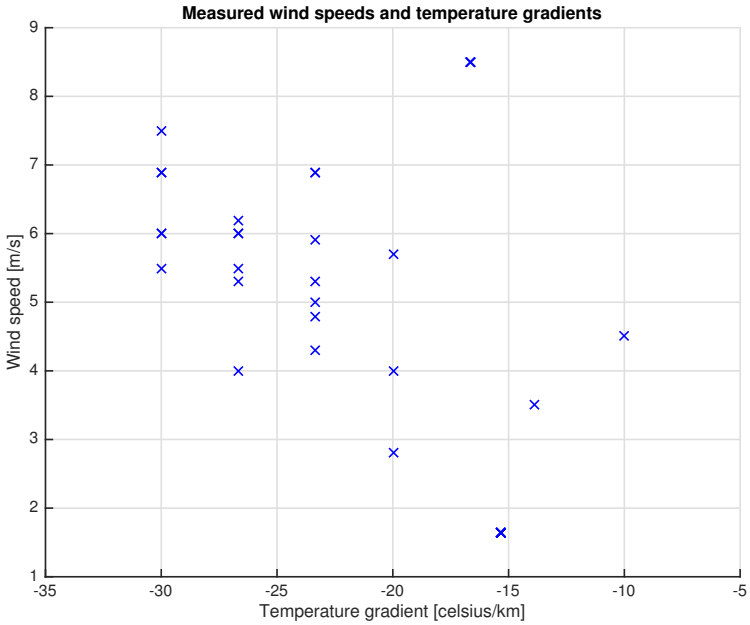

Figure 24: Measured wind speeds and temperature gradients. The negative temperature gradient seemed to have some correlation with increasing wind speeds.

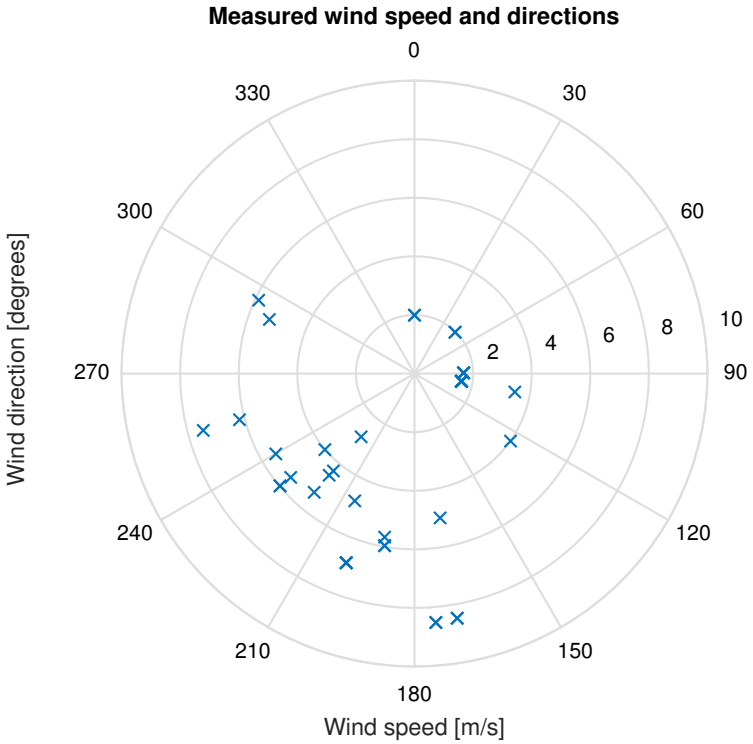

Figure 25: Measured wind speeds and corresponding wind directions. The majority of the measured wind speeds were over $4\frac{m}{s}$, from directions between 150° and 270°

5.1.2 Total sound exposure levels and charges

The stated charges that were detonated during the measurements varied between 11kg...224kg, and most of them were between 45kg...82kg. The C-weighted exposure levels L_{CE} at the measurement location (4km) varied between 77dB...106dB.

In Figure 26 the different charges in kilograms are compared to the corresponding exposure levels measured at the receiver. The data shows that the variation in L_{CE} were around 20dB for a charge size around 50kg, and between 45kg...82kg the spread remains approximately the same. Most of the measured exposure levels are below the L_{CE}=100dB guideline value. However, at charge sizes above 100kg, this value was exceeded in most of the measurements.

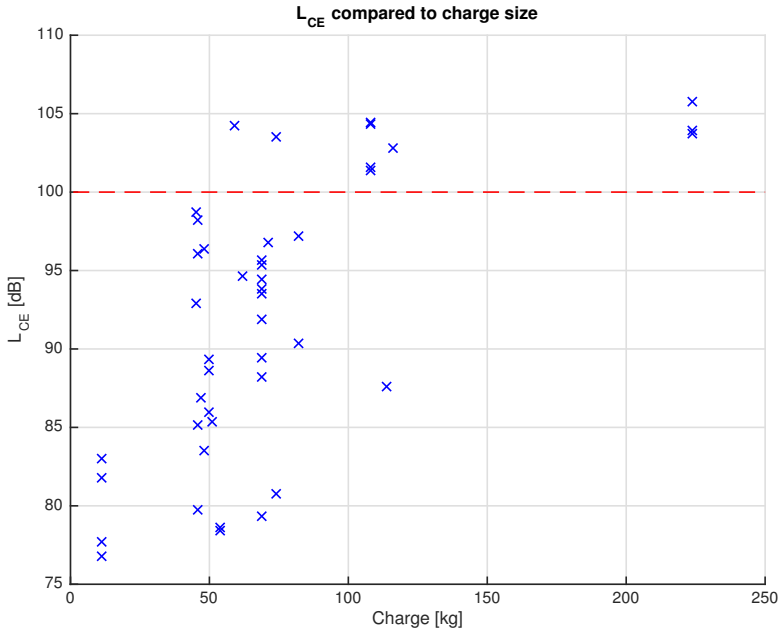

Figure 26: Measured L_{CE} exposure levels and corresponding charges. As can be seen, the spread in L_{CE} is about 20dB for charge size around 50kg.

5.1.3 Total sound exposure levels in different meteorological conditions

Wind speed component

Figure 27 shows the measured exposure levels L_{CE} compared to the wind speed component parallel to the receiver direction. The different exposure levels are plotted in the groups of different size of charges in order to minimize the effect of the charge and on the other hand to emphasize that the over 100kg charges seem to result in higher exposure levels. It can be seen that the L_{CE}=100dB guideline value exceeds mostly within the 100kg...224group group. Unfortunately, the most of the measurements in this group are measured under downwind conditions, so the correlation between the L_{CE} and wind speed cannot be seen in this group.

The 45kg...82kg charge range, which was the biggest group in the conducted measurement period, seems to have smaller noise levels under the upwind conditions and higher during downwind, as stated in the theory section. The smallest charge group (four measurements), 11kg, shows the lowest exposure levels and no clear correlation with wind speed.

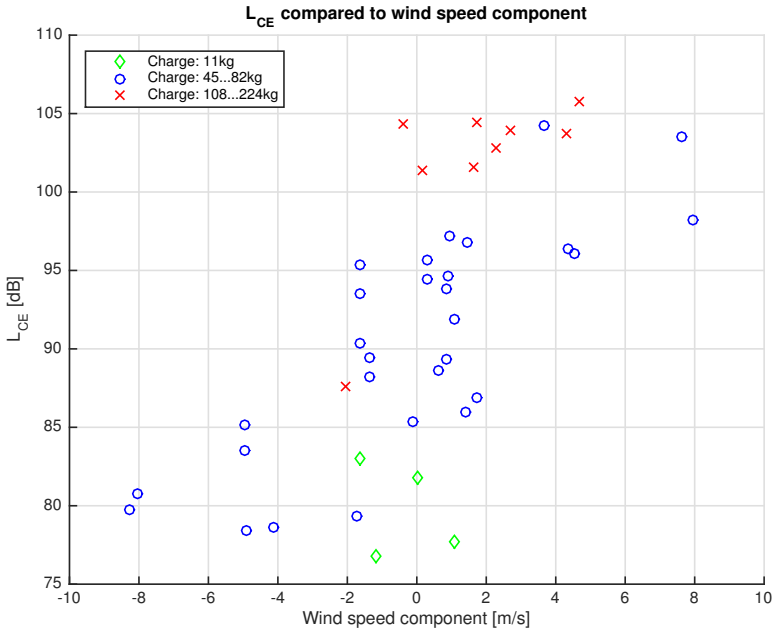

Figure 27: The measured exposure levels L_{CE} compared to corresponding wind speed component. In order to minimize the possible effect of the charge size the data is plotted in three charge groups. This data set includes some older measurements from the same site.

In comparison, not forgetting the relatively small amount of data, only the data from the original measurement point of this thesis is plotted in the Figure 28. The correlation here between the upwind conditions and the attenuation of sound is more clear, and the spread under similar wind conditions is around 11dB. This data set also includes a few over 100kg charges (resulting most of the L_{CE} $\geq$100dB exposure levels), but they are mostly in line with the new measurements.

Figure 29 shows all the measurements together. As can be seen, within all charge groups it is a slightly more difficult to find the correlation between the exposure level and the wind speed. Under similar conditions there is a spread of about 20dB (around $\pm 2\frac{m}{s}$) between the highest and lowest measured values. Still, the correlation between the upwind conditions and attenuation is clear.

In Figure 30 the A-weighted exposure levels L_{AE} are presented. As can be noticed, the trend is similar to C-weighted levels presented for example in Figure 27. The sound exposure levels L_{AE} are notably lower when compared to L_{CE} as A-weighting attenuates more on low frequencies. Note, that L_{AE} is generally used for calculating daytime L_{eq} in case of multiple explosions per day.

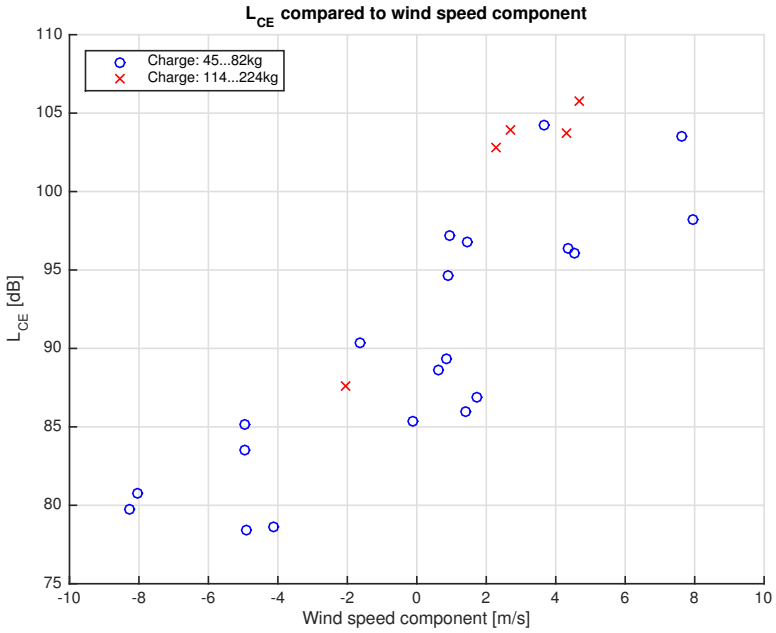

Figure 28: The measured exposure levels L_{CE} compared to corresponding wind speed component. The possible effect of the charge size is minimized plotting the data in different charge groups. The amount of the data is relative small, but large enough for illustrating the effect of the wind.

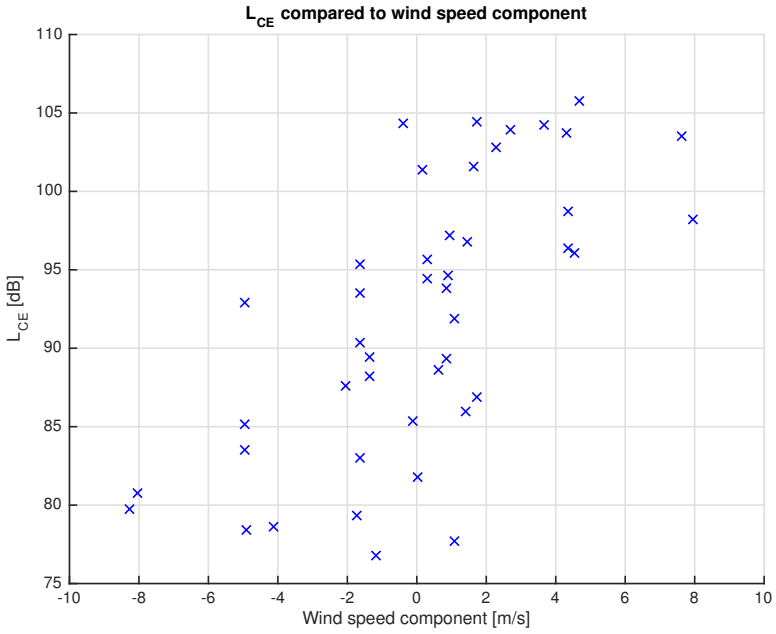

Figure 29: Total exposure levels L_{CE} gathered from the whole data set compared to corresponding wind speed components. The large variation in L_{CE} around wind speeds of $\pm 2 \frac{m}{s}$ is notable.

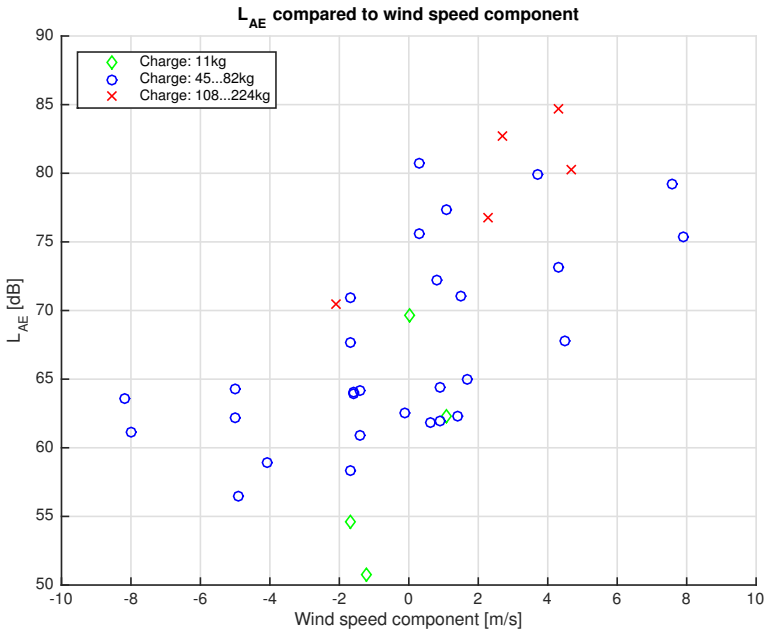

Figure 30: Total exposure levels L_{AE} gathered from the whole data set compared to corresponding wind speed components. Similar trend can be noticed when compared to C-weighted levels presented e.g. in Figure 27.

Temperature gradient

The effect of the temperature gradient on exposure levels does not show any clear correlation, as illustrated in the Figure 7. Similar levels were obtained in all the conditions during the measurements, and the dispersion during the same temperature conditions seems to be around 20dB at largest. Note, that the old measurements with no temperature gradient information are not included.

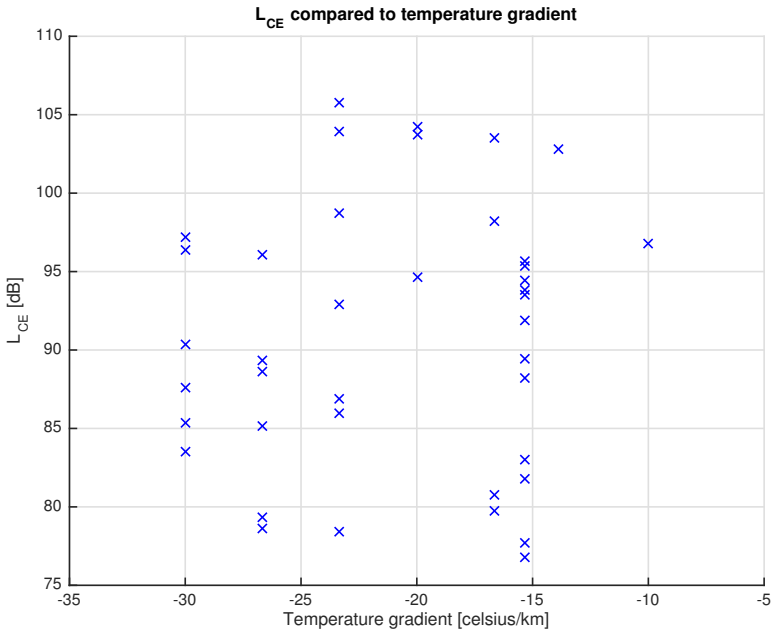

Figure 31: Measured temperature gradient compared to the sound exposure level L_{CE}.

Even though the exposure levels are plotted in the charge ranges in order to minimize the effect of the charge, there cannot be found any noticeable correlation within the groups and the temperature gradient. Also, due to the limited amount of weather conditions the combined effect of the wind speed component and the temperature gradient cannot be stated.

5.1.4 One third octave spectrum analysis

An example of the measured blast impulse waveform and its third octave spectrum with different frequency weightings is presented in the Figure 32. The shape of the waveform is similar to the earlier mentioned Friedlander waveform, and the effect of the ground reflections can be seen as dips and peaks in the spectrum. It is notable that at very low frequencies the recorded blast has a significant amount of energy, even at the point of measurement, that is four kilometers from the source.

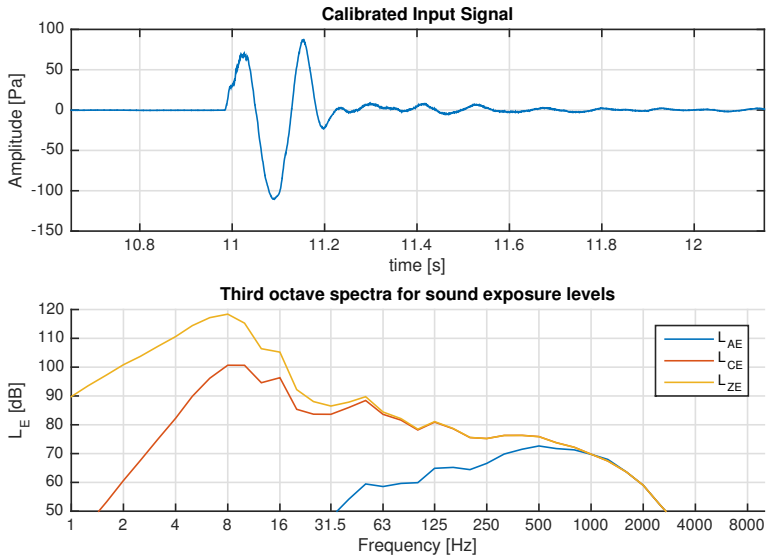

Figure 32: An example of a recorded blast. Above the time signal is illustrated and below the corresponding exposure spectra in one third octave bands. As can be noticed from the unweighted spectrum (L_{ZE}), the blast has a significant amount of energy at very low frequencies. The effects of the A and C frequency weightings are well illustrated here, when L_{CE} and L_{AE} are compared to the original linear spectrum. The wide band total exposure levels are: L_{ZE}=123.2dB, L_{CE}=105.8dB and L_{AE}=80.2dB.

In the Figure 33 the ambient background noise spectrum (L_{ZE}) is plotted and compared against corresponding blast. The level difference (SNR) is also shown with frequency. The background noise is analyzed from a recorded wave file 9 seconds after the blast, with a duration of 9 seconds. Between the 12.5Hz and 125Hz one third octave bands the noise levels (L_{ZE}) are about 20dB higher than the background. Below 12.5Hz the difference is over 30dB. The peak found in the background noise at 100Hz is most probably noise from a generator located close to the recording site. Hereby, the background noise does not affect the total sound exposure levels.

In Figure 34 two measured blast pair spectra are plotted under opposite wind conditions. In the first plot, the calculated wind speed component was about $\pm 4\frac{m}{s}$ and charge about 50kg, and below the corresponding values around $\pm 2\frac{m}{s}$ and 115kg. As can be seen, the wind conditions attenuate all the frequencies approximately in the same scale, and remarkable deviations cannot be found.

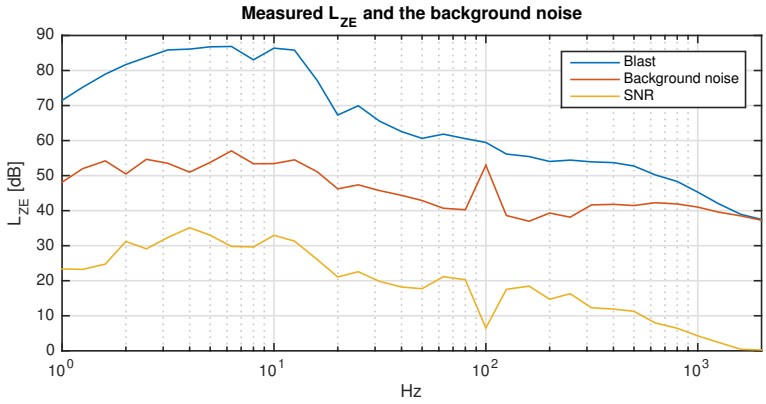

Figure 33: An example of a recorded blast and background noise. The biggest difference, about 30dB, is found below 12.5Hz. Between 12.5...125Hz the difference is around 20dB. The peak found in the background noise is probably caused by a nearby generator.

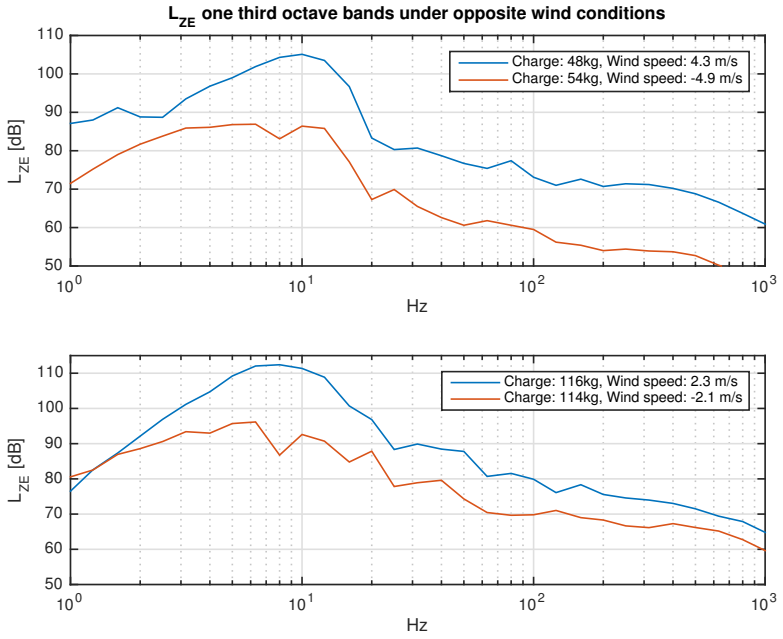

Figure 34: One third octave band spectra (L_{ZE}) of two blast pairs measured under similar conditions. The upwind propagation conditions attenuate all frequencies approximately in a same manner.

All the measured linear one third octave spectra are plotted in the Figure 35. There can be seen that the highest peaks can be found at very low frequencies, and the spectra of the blasts are similarly shaped.

The highest spectral peak frequencies are compared to detonated charge in Figure 36. As stated in theory, in context of the sound source approximation applying Weber spectrum, the largest charges cause spectral peaks at the lowest frequency

bands. However, occasional peaks at equally low frequency bands are also obtained with smaller charges.

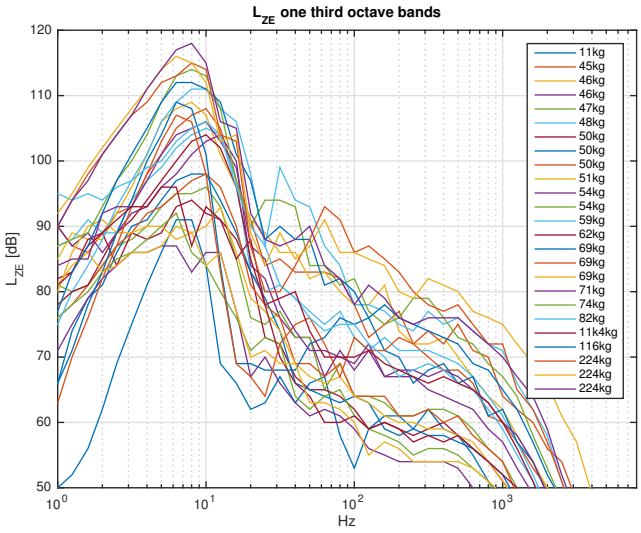

Figure 35: Linear one third octave spectra of each blast. The highest peaks are obtained around 10Hz and obtained with 224kg charge. Below 224kg the highest peaks are obtained with charges 45kg...116kg more randomly.

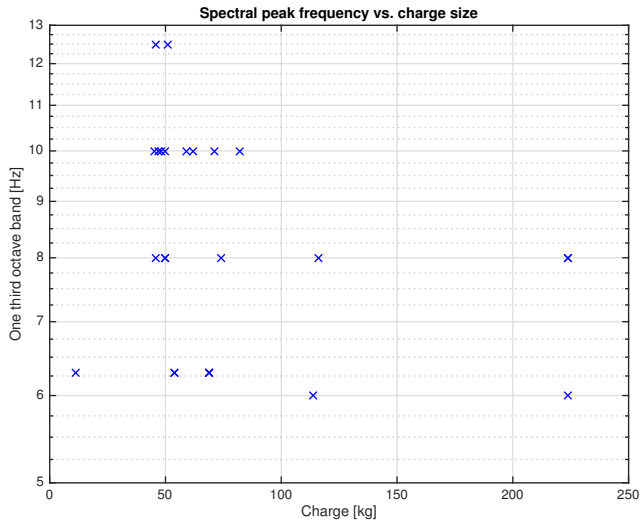

Figure 36: The highest one third octave band peaks compared to the corresponding charge in kilograms. The spread around 50kg charge is largest (6.3Hz...12.5Hz), but over 100kg charges seem to cause peaks at 8Hz and under.

5.2 Predictions using Nord 2000

The measured blasts were replicated using Nord 2000 propagation model in the Cadna Software. Only the measurements measured in the original receiver point were modeled. The predictions of the old measurements are not included due to limited weather data.

5.2.1 Calculations results in comparison with the charge

The calculations give similar results in L_{CE} compared to measurements, but the spread is around 13dB for all the calculations. As can be observed from the Figure 37, about 10dB spread can be obtained around 50kg charge and the highest levels are obtained with 224kg charge.

The results are similar to the measurement results, even though the spread is notably smaller. This may be due to the fact that the sound propagation path in the real world has instabilities like turbulence causing dispersion, which is not taken into account in the calculations. Also, the source emission is an approximation, and the distance between source and the receiver is also longer than the model is designed for.

Interestingly enough, almost all of the calculated sound exposure levels L_{CE} are somewhat over 100dB, which is not in the line with measurements. This aspect is covered later in this section.

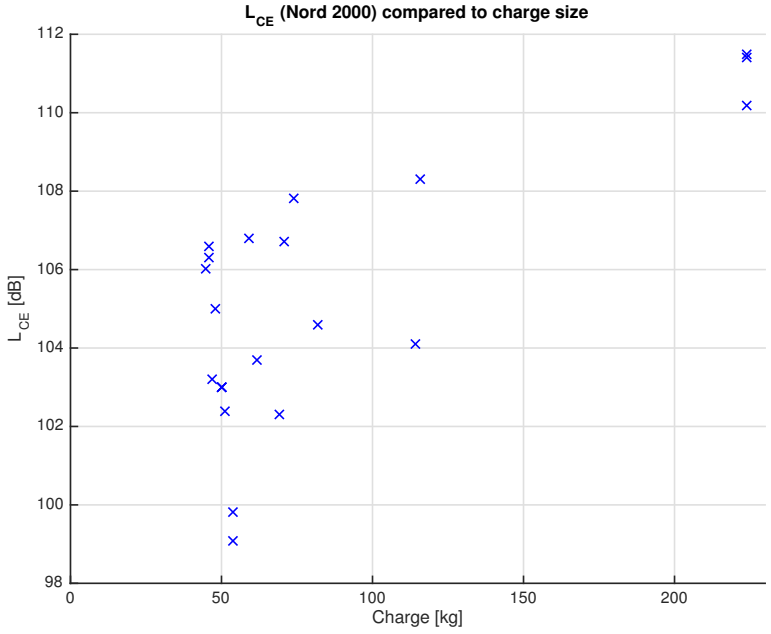

Figure 37: L_{CE} calculation results from the Nord 2000 prediction model compared to corresponding charge. Similarities to measurements are clear.

5.2.2 The effect of the weather

Wind speed component

The prediction results compared to wind speed adhered to the theory and also the measurements, as can be seen in Figure 38. The prediction model gives smaller exposure levels in upwind than in the downwind conditions, as expected. The effect of the wind on the sound propagation seems to be more clear here than in the measurements, and as stated before, the spread between the exposure levels is smaller.

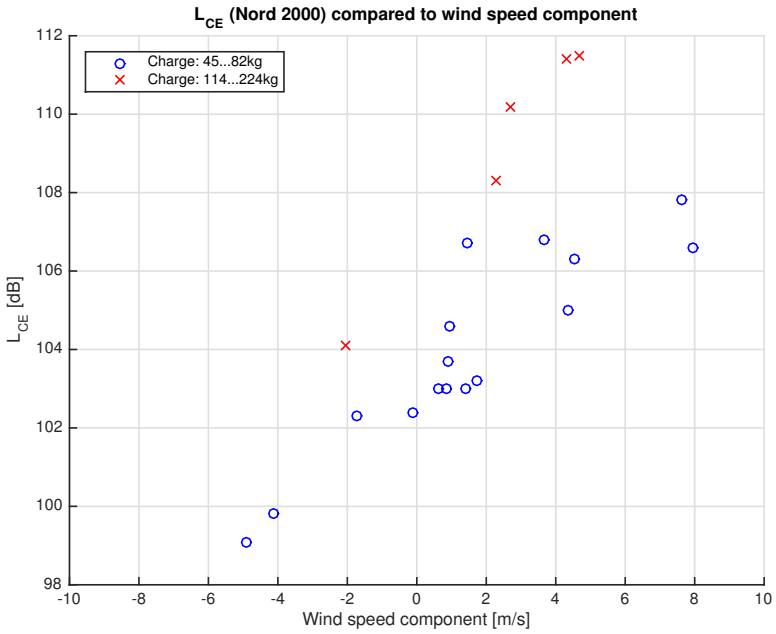

Figure 38: Predicted exposure levels L_{CE} compared to the corresponding wind speed component parallel to the sound propagation path. Under upwind sound propagation conditions the prediction results are smaller compared to downwind conditions, as expected.

Like before, the presented (prediction) results are divided into charge groups. It seems that the prediction scheme follows more linearly the wind speed, and the spread here is only a few decibels under similar wind conditions.

Temperature gradient

The L_{CE} compared to temperature gradient did not show any clear correlation, as can be seen from the Figure 39. This is completely in line with the observations done in the measurement analysis. The absence of the inversion or positive temperature gradient would maybe result some correlation, but as shown in theory (e.g. in Figure 12), the results would not be remarkable at least in C-weighted levels.

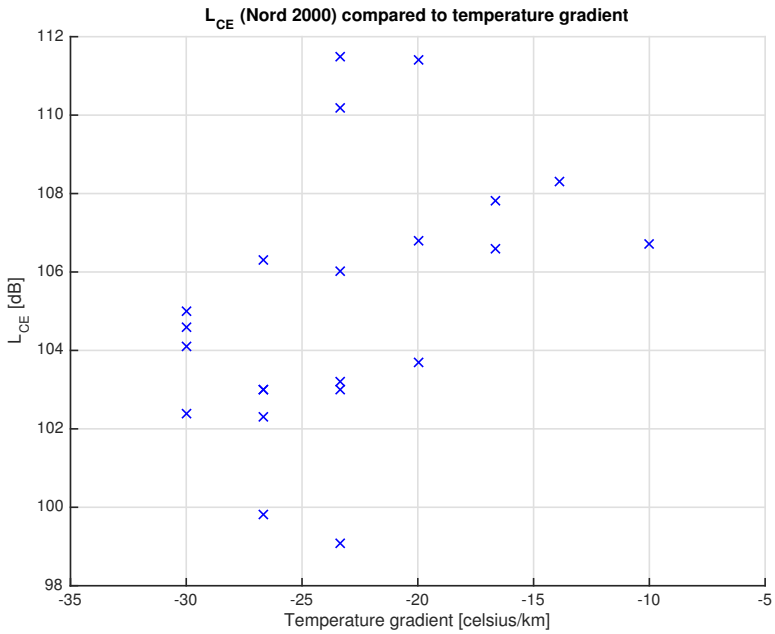

Figure 39: Predicted exposure levels L_{CE} compared to corresponding temperature gradient. No clear correlation between the temperature gradient and the L_{CE} can be found.

5.2.3 Measurements compared to the predicted sound exposure levels

In the Figure 40 the difference between the measured and the predicted sound exposure levels are presented with corresponding wind components. Here the predicted values are subtracted from the measured values resulting the difference in decibels. The variation between the predicted and measured exposure was about -10...+5dB in L_{ZE} and -23...-4 in L_{CE}, respectively. Two major observations can be made:

- Larger differences can be found under the upwind sound propagation conditions (prediction gives larger values)

- The linear sound exposure level L_{ZE} is closer to the measured level in all cases

The biggest differences are obtained under upwind conditions, so it seems that wind causes less attenuation in the model than in reality. Also, the enhancement caused by downwind conditions seems to be smaller.

Dispersion in the measurements can also be observed here. As stated previously, the prediction follows more linearly the effect of the wind, and the spread in L_{CE} modeled under the same wind conditions was remarkably smaller than in the measurements. The variations in difference between wind speeds close to each other are most probably caused by the dispersions (i.e. the instabilities on the physical sound propagation path) in the measurements.

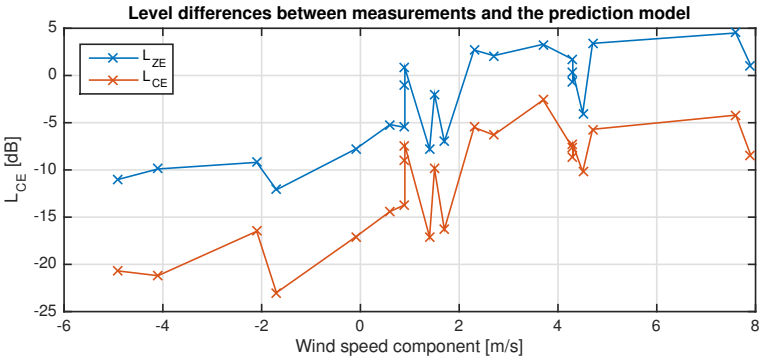

Figure 40: Level differences between measurements and the prediction model at various wind speeds. The difference is biggest under upwind conditions and the predicted L_{CE} seems to give higher level through out the data set.

In the Figure 41 an example of measured and predicted noise levels are shown in octave bands under upwind conditions. The illustrated case is the first pair from the data sequence in Figure 40. As can be seen the prediction results show significantly higher noise levels at low frequencies and lower levels at high frequencies. The difference at high frequencies is due to measured ambient background noise that is also plotted in the same figure. CadnaA and prediction methods do not take background noise into an account at any level, in other words, the prediction scheme calculates only the noise levels caused by the source emission.

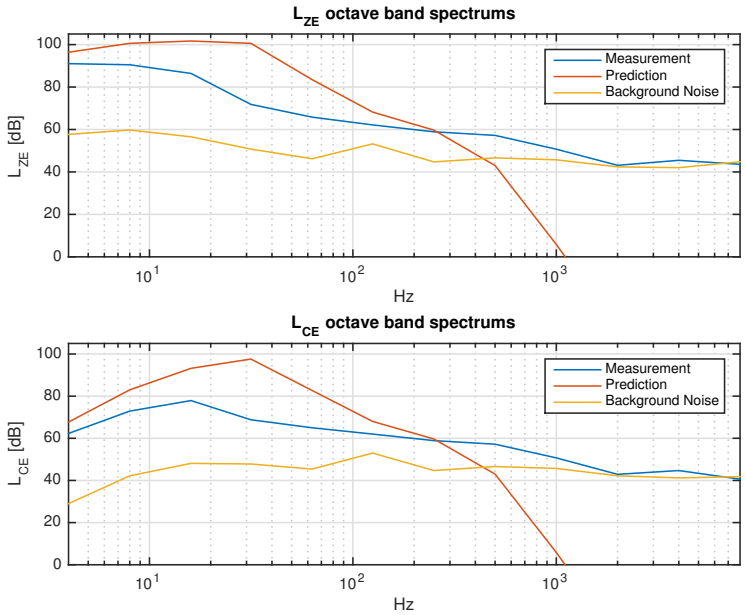

Figure 41: Octave spectra of measured and predicted noise levels (L_{ZE} and L_{CE}) together with the background noise. As can be seen, the level above 1000Hz drops to zero and below, this is due to absence of the background noise. On lower frequencies, the prediction shows higher levels compared to the measured spectra.

5.3 Sources of error

In addition to the earlier mentioned errors caused by equipment, every measurement has some amount of error caused by extrinsic factors. When it comes to the measurements in this thesis and applying the results elsewhere, one important factor is the fact that the measurements are mostly performed at a single measurement point. Although the sound propagation path stays constant, different results may be obtained at some other point at the same distance, and under exactly the same conditions. Long distances cause uncertainty, for example, turbulence or rapid wind speed changes are possible within the propagation path.

All the measurements were performed in late spring or summer time when sun rises early in the morning, hours before the detonations. The possible inversion would have been most probably during those hours. The atmospheric temperature profiles are different from autumn and winter time [24], and also snow has an effect on the ground level temperature and the ground effect.

The temperature profile or gradient measured from the 40 meters high mast may be not accurate enough at such long distances (several kilometers). The layers of air may have different temperatures at different altitudes and also change among the propagation path. This is not measurable with available equipment, as the height of the mast is limited. In addition, the (averaged) parameter taken from the meteorological station may also cause some error to the results: choosing different average or the instant values, the results would differ, especially at long distances where the variation on the propagation path cannot be measured. The earlier mentioned error caused by the temperature sensors is not seen noteworthy in the conducted measurements as variation in the sound exposure levels was found out to be large. However, if a positive temperature gradient was found, the error caused by the sensor could have notable effect, but this cannot be verified here.

In the measurement analysis, also the wind direction may cause dispersion. The wind speed component parallel to the propagation path does not take side wind into account. The downwind or upwind component is calculated using cosine, thus 90 degrees wind direction is taken as $0\frac{m}{s}$. In theory, the side wind not is seen having effect on the sound propagation, but from these measurements this cannot be verified.

Also, the additional data borrowed from the old measurements causes some dispersion. The distance correction does not take the ground and the obstacles into an account. Though, the topography is almost flat in Ähtäri. In addition, the reported weather data is from Finnish Meteorological Institute (FMI) and it is not an accurate condition for the blast site, but an estimate for the greater area of Ähtäri.

Another major factor are the charges used in the explosions. The material that is being disposed of, and the additional explosive material itself are not precisely known, and it is not possible to normalize the amount e.g. to TNT or equivalent. This may cause spread in the source emission, as for example 70kg of an unstated explosive material may have a different *relative effectiveness factor* (R.E. factor, i.e. the amount of TNT equivalent to the same demolition power) compared to another charge with the same amount in mass.

In the propagation modeling, one of the major errors is the calculation of the

source emission. In this thesis, the sound emission L_w for the explosions is an approximation obtained using the Weber spectrum, assuming that the explosive compound is TNT. Note, that the Weber spectrum was not originally designed to be used as an approximation for the charge sizes presented in this thesis [48].

Changes in the terrain model may have a major effect on the results. For example, moving the source or receiver few dozen meters may cause over remarkable difference between two calculations in the same conditions if there is an obstacle in direct line between the source and the receiver. This is be due to the fact that the software calculates rays between two points. That means, the exact location of the source and the receiver are important in order to get results comparable to the measurements. In addition the model is not designed to be used or to be accurate at such large distances that are investigated in this thesis.

6 Conclusions

In this thesis the effects of varying meteorological conditions on the propagation of impulsive noise at long distances was researched. In order to gather data, a sound level meter was set up at Finnish Defence Force's explosives demolition center in Ähtäri. The measurements were conducted according to the guidelines used for measuring noise emitted by heavy weapons and explosions [15]. For measuring the meteorological conditions, a weather station has been set up on the site by the FDF. Key findings of this thesis were:

- The weather conditions have a clear effect on the noise emissions
- The wind component parallel to the sound propagation path seems to be the dominant parameter
- There is a large variation in the measurement results even in the similar conditions with similar sized charge
- Noise modeling can be used for estimating noise levels and applied as a prediction tool within some limits
- As guideline, under 100kg charges cause L_{CE} $\leq$100dB noise levels at four kilometers from the blast under all weather conditions at least when negative temperature gradient occurs

The blasts were recorded with the sound level meter, and for analysis, a Matlab tool was developed. Motivation for the tool was to be able to analyze one third octave spectra down to infrasound bands, starting from 1Hz. The tool was found out to be found out to be accurate in comparison with professional reference software.

The measured sound exposure levels showed a large variation between measurements (about 20dB), even under similar weather conditions. The charge seemed to have a minor effect on the measured exposure levels, but it is not completely clear as the most of the charges were within the same range (45...82). In most cases charges under 100kg charges resulted as exposure levels under L_{CE} =100dB guideline value, while larger charges exceeded it. The distance to the blast site was about 4000 meters.

As expected, the meteorological conditions were found to have a correlation with the measured exposure level L_{CE}. The wind speed and the temperature gradient seem to be inversely proportional to each other, as stated in the theory. No clear correlation was found between the temperature gradient and the measured exposure level, while the correlation with the wind speed component was clear.

The wind speed component parallel to the sound propagation path seemed to be the dominant parameter, noting the fact that during the conducted measurements

positive temperature gradient was not found at all. Still, the results seem to follow the pattern where the lowest exposure levels can be obtained during a combination of upwind and strong negative temperature gradient, as shown in the theory.

The sound propagation prediction using the Nord 2000 model resulted similar trends as measurements. The predicted exposure levels were higher under downwind conditions and lower under upwind, respectively. The spread under similar conditions was smaller compared to the measurements, this may be due to the fact that the physical sound propagation path has instabilities (e.g. turbulence) that are not included in the prediction.

The differences between the measured and predicted exposure levels (L_{ZE} and L_{CE}) were bigger under upwind propagation conditions. Nord 2000 resulted in 10dB (L_{ZE}) and 20dB (L_{CE}) higher levels at highest compared to the measured levels. On the other hand, the prediction gave 5dB smaller values (L_{ZE}) at highest under downwind. It seems that the wind attenuates the sound more in nature than in the model, but also enhances it more.

As conclusion to the noise modeling, the Nord 2000 prediction scheme can be applied as a tool in order to predict noise levels under various weather conditions and even at long distances. An accurate result is not likely to be achieved, but as the prediction results seem to be higher under upwind sound propagation conditions, a safe approximation could be achieved by subtracting about 15dB from the predicted sound exposure levels (L_{CE}) under these conditions and perhaps about 5 dB under neutral and favorable conditions.

As answers to the main research questions; the meteorological conditions have high enough effect on the outdoor sound propagation for noise abatement purposes. This was verified by measurements and predictions. The magnitude of the weather effect cannot be stated with great confidence due to the large variation in a relatively small amount of data, but as guidelines can be stated that under upwind conditions, with charges under 80kg, the resulting L_{CE} will stay under the 100dB guideline value at distance of four kilometers.

6.1 Future work

Referring to the theory, predictions and conducted measurements, a tool proper for estimating noise levels in Ähtäri could be developed. On the other hand, in order to apply the results in other FDF's activities, more measurements and larger amounts of data would be recommended to be gathered in order to:

- Achieve more precise knowledge about temperature profiles and their effect on the sound propagation

- Get more information about up- or downwind conditions compared to sidewind conditions

- Attain better resolution with comparable charge sizes

- Gain more accurate tools to predict noise levels at residential areas

Continuous measurements through a year would give not only remarkably larger amount of data but also data from all the seasons. By this the different temperature profiles could be evaluated, and most probably the best season for detonation activities would be found.

The further measurements should also have more measurement points, at least two opposite points at same distance in reference to the emission. By this the upwind and downwind conditions for the same blast could be evaluated more precisely. If taken one step further, using four measurement points would present the sidewind conditions and so all the different wind directions could be evaluated.

Another interesting point of view would be documenting and calculating the exact amounts of explosive compound in order to have a charge normalized to e.g. TNT. The blast measurements should be conducted using approximately same sized charge to minimize the dispersion.

If these actions were executed a more accurate tools for predicting the noise emissions at nearby residential areas could be developed. This kind of extensive knowledge could be also applied further and expanded to be used not only in one location and activity, but also on other sites and activities that cause remarkable amounts of noise over long distances.

References

[1] Lahti, T. Akustinen mittaustekniikka. 2. painos. Espoo, Teknillinen korkeakoulu, Sähkötekniikan osasto, Akustiikan ja äänenkäsittelytekniikan laboratorio, 1995.

[2] Attenborough, K., Li, M. K., Horoshenkov K. Predicting Outdoor Sound. 2007. ISBN: 0-419-23510-8

[3] ISO 9613-1:1993 *Acoustics - Attenuation of sound during propagation outdoors - Part 1: Calculation of the absorption of sound by the atmosphere*International Organization for Standardization.

[4] Rossing, T. D. The Science of Sound. 2nd Edition. 1990. ISBN: 0-201-15727-6

[5] Karjalainen, M. Kommunikaatioakustiikka. Espoo, Aalto-yliopisto, Sähkötekniikan korkeakoulu, Signaalinkäsittelyn ja akustiikan laitos, 2011. ISBN: 978-952-60-4049-3

[6] ISO 1996-1:2003 *Acoustics - Description, measurement and assessment of environmental noise - Part 1: Basic quantities and assessment procedures*International Organization for Standardization.

[7] ISO 226:2003 *Normal equal-loudness-level contours*International Organization for Standardization.

[8] IEC 61672-1:2013 *Electroacoustics - Sound level meters - Part 1: Specifications* Geneva, Switzerland. International Electrotechnical Commission, 2013.

[9] Jokitulppo, J., Lahti, T., Markula, T. Ampumamelun arviointi *Ympäristöministeriö*, 2007.

[10] Kerry, G., Ford, R. D. and James D. Bandwidth Limitation Effects on Low-Frequency Impulse Noise Prediction and Assessment. *Applied Acoustics* 1996, vol. 47, nro 4, pp. 331–344.

[11] Zwislocki, J. J. Temporal Summation of Loudness: An Analysis. 1969 *The Journal of the Acoustical Society of America.* pp. 431–441.

[12] Florentine, M., Buus, S., Poulsen, T. Temporal integration of loudness as a function of level. 1995 *The Journal of the Acoustical Society of America.* pp. 1633–1644.

[13] Valtioneuvoston päätös 993/1992 *Valtioneuvoston päätös melutason ohjearvoista* 29.10.1992.

[14] Valtioneuvoston päätös 53/1997 *Valtioneuvoston päätös ampumaratojen aiheuttaman melutason ohjearvoista* 16.1.1997.

[15] Jaloniemi, J., Pääkkönen, R., Parri A. Raskaiden aseiden ja räjähteiden aiheuttaman ympäristömelun arviointi *Puolustusvoimien ohje* 2005

[16] Valtioneuvoston asetus 85/2006 *Valtioneuvoston asetus työntekijöiden suojelemisesta melusta aiheutuvilta vaaroilta*

[17] Asumisterveysopas - Asumisterveysohjeen soveltamisopas *Sosiaali- ja terveysministeriö* 2003. ISBN 952-9637-30-6

[18] Asumisterveysohje - Asuntojen ja muiden oleskelutilojen fysikaaliset, kemialliset ja mikrobiologiset tekijät *Sosiaali- ja terveysministeriö* 2003. ISBN 952-00-1301-6

[19] Delany, M. E., Bazley, E. N. Acoustical Properties of Fibrous Absorbent Materials. *Applied Acoustics.* England, 1970.

[20] Aalto, M., Oskarson, J. *Sound and Vibration measurements - Measurement of sound outdoors*, Chalmers University of Technology. 2013.

[21] Huseby, M., Rahimi, R., Teland, J. A., Dyrdal, I., Fykse, H., Hugsted B., Wasberg C. E., Final report: Improvement of the computational methods of the Norwegian Defence Estates Agency for computing noise from the Norwegian defence training ranges. *Norwegian Defence Research Establishment.* Norway, 2007.

[22] Lahti, T. Äänen eteneminen maan pinnalla. Espoo, Helsingin Teknillinen korkeakoulu, Akustiikan laboratorio. Julkaisu n:o 16. 1979. ISBN: 951-751-535-9

[23] Bruel & Kjaer Sound & Vibration Measurements A/S. *Environmental Noise.* 2001.

[24] Maijala, P. A measurement-based statistical model to evaluate uncertainty in long-range noise assessments. *VTT Technical Research Centre of Finland* Dec 2013. ISBN 978-951-38-8109-2

[25] Renez Nota, Robert Barelds, Dirk van Maercke. *Harmonoise WP 3 Engineering method for road traffic and railway noise after validation and fine-tuning.* No. Deliverable 18. (2005).

[26] Markula, T., Peltonen, T., Lahti T. Ammunnan ja räjäytysten aiheuttama tärinä *Insinööritoimisto Akukon Oy* Helsinki, 2009

[27] Madshus, C., Nilsen, N., I. Low Frequency Vibration and Noise From Military Blast Activity: Prediction and Evaluation of Annoyance. *The 29th International Congress and Exhibition on Noise Control Engineering.* 2000 ,Nice, France.

[28] Madshus, C., Lovholt, F., Kaynia, A., Hole, L. R., Attenborough, K., Taherzadeh S. Air-ground interaction in long range propagation of low frequency sound and vibration - Field tests and model verification. *Applied Acoustics*. 2004, vol. 6, pp. 553-578.

[29] B&K - 2250 Sound Level Meter - Type 2250 http://www.bksv.com/Products/handheld-instruments/sound-level-meters/sound-level-meters/type-2250.aspx

[30] B&K - Sound Calibrator - Type 4231 http://www.bksv.com/products/transducers/acoustic/calibrators/4231

[31] B&K - Half-inch free-field microphone, 6.3 Hz to 20 kHz, prepolarized - 4189 http://www.bksv.com/Products/transducers/acoustic/microphones/microphone-cartridges/4189?tab=overview

[32] B&K - Outdoor microphone kit - UA-1404 http://www.bksv.com/products/transducers/acoustic/microphones/microphone-preamplifier-combinations/4198

[33] Sustainability of Digital Formats Planning for Library of Congress Collections http://www.digitalpreservation.gov/formats/fdd/fdd000001.shtml

[34] Vaisala HMP155 Humidity and Temperature Probe *Data sheet*

[35] Vaisala DTR13 Radiation Shield *Data sheet*

[36] Vaisala Temperature Sensor *Data sheet*

[37] Vaisala WAA252 Heated Anemometer *Data sheet*

[38] Vaisala WMT700 WINDCAP Ultrasonic Wind Sensor *Data sheet*

[39] Vaisala Automatic Weather Station AWS130 *Data sheet*

[40] Ympäristömelun mittaaminen *Ympäristöministeriö* 31.1.1995. ISBN 951-731-082-X

[41] Ampumaratamelun mittaaminen, Ympäristöopas 61 *Ympäristöministeriö* 1999. ISBN 052-11-0496-1

[42] Ympäristömelun arviointi ja torjunta, Ympäristöopas 101 *Ympäristöministeriö* 2003. ISSN 1238-8602

[43] ISO 1996-1-3:2003 *Acoustics - Description, measurement and assessment of environmental noise*International Organization for Standardization.

[44] Kragh, J., Andersen, B., Jakobsen J. Environmental Noise from Industrial Plants. General Prediction Method *Danish Acoustical Laboratory*, 1982

[45] Kragh, J., et. Al. Nordic Environmental Noise Prediction Methods, Nord2000 Summary Report. General Nordic Sound Propagation Model and Applications in Source-Related Prediction Methods *Danish Electronics, Light and Acoustics*, 2002.

[46] Klinkby, J.,. Nord200 vs. the Existing Nordic Propagation Models *Danish Electronics, Light and Acoustics*, 2002.

[47] DataKustik GmbH - CadnaA http://www.datakustik.com/

[48] ISO 17201-2 *Acoustics - Noise from shooting ranges - Part 2: Estimation of muzzle blast and projectile sound by calculation*International Organization for Standardization, 2006.

[49] Sääolot ympäristömelun laskentamalleissa, Suomen Ympäristö 655 *Ympäristöministeriö* 2003. ISBN 952-11-1517-3

[50] Zouboff, V., Brunet, Y., Berengier, M., Sechet, E. A qualitative approach of atmospheric effects on long range sound propagation. *6th International Symposium on Long Range Sound Propagation.* 1994, Ottawa, Canada, pp. 251-269.

[51] Adobe Audition - Adobe Systems Incorporated. https://creative.adobe.com/fi/products/audition

[52] Octave Toolbox by Couvreur C. http://www.mathworks.com/matlabcentral/fileexchange/69-octave

[53] Couvreur C. Implementation of a One-Third-Octave Filter Bank in Matlab.

[54] IEC 1260 *Electroacoustics - Octave-band and fractional-octave-band filters* Geneva, Switzerland. International Electrotechnical Commission, 1995.

[55] imc Meßsysteme GmbH http://www.imc-berlin.com/products/measurement-software/imc-famos/

[56] IEC 61260-1 *Electroacoustics – Octave-band and fractional-octave-band filters – Part 1: Specifications* International Electrotechnical Commission, 2014

[57] Pioneer Hill Software LLC - Spectra Plus http://spectraplus.com/

[58] Microsoft Excel https://products.office.com/en-us/excel?legRedir=true&CorrelationId=2e72245c-8358-43a4-8cc2-e89de9abea94

[59] Parri, A. Ympäristömelumittaus Ährärin Palolammen Räjäytyksistä *Itäisen Maanpuolustusalueen Esikunta* Mikkeli, 2007.

[60] 01dB Duo Smart Noise Monitor http://01db.acoemgroup.com/catalog/01dB-DUO-Smart-Noise-Monitor

A Map of the Palolampi area

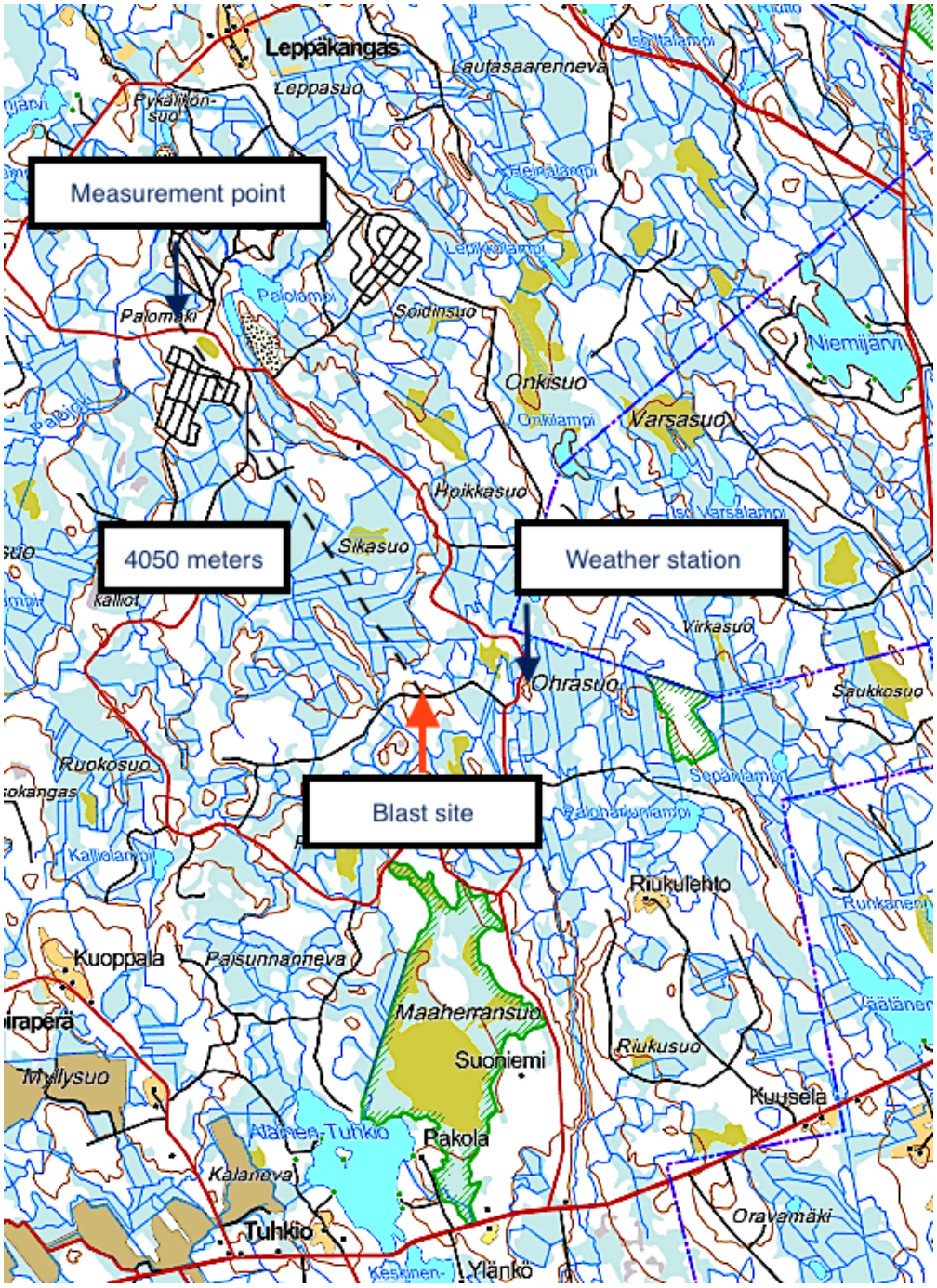

Figure A1: A map of the Ähtäri measurement site. The measurement point, the weather station and the blast site are marked in the map with arrows. The dashed line illustrates the direct path from blast site to measurement point. The map is taken from National Land Survey of Finland (Maanmittauslaitos).

B Illustration of the weather mast

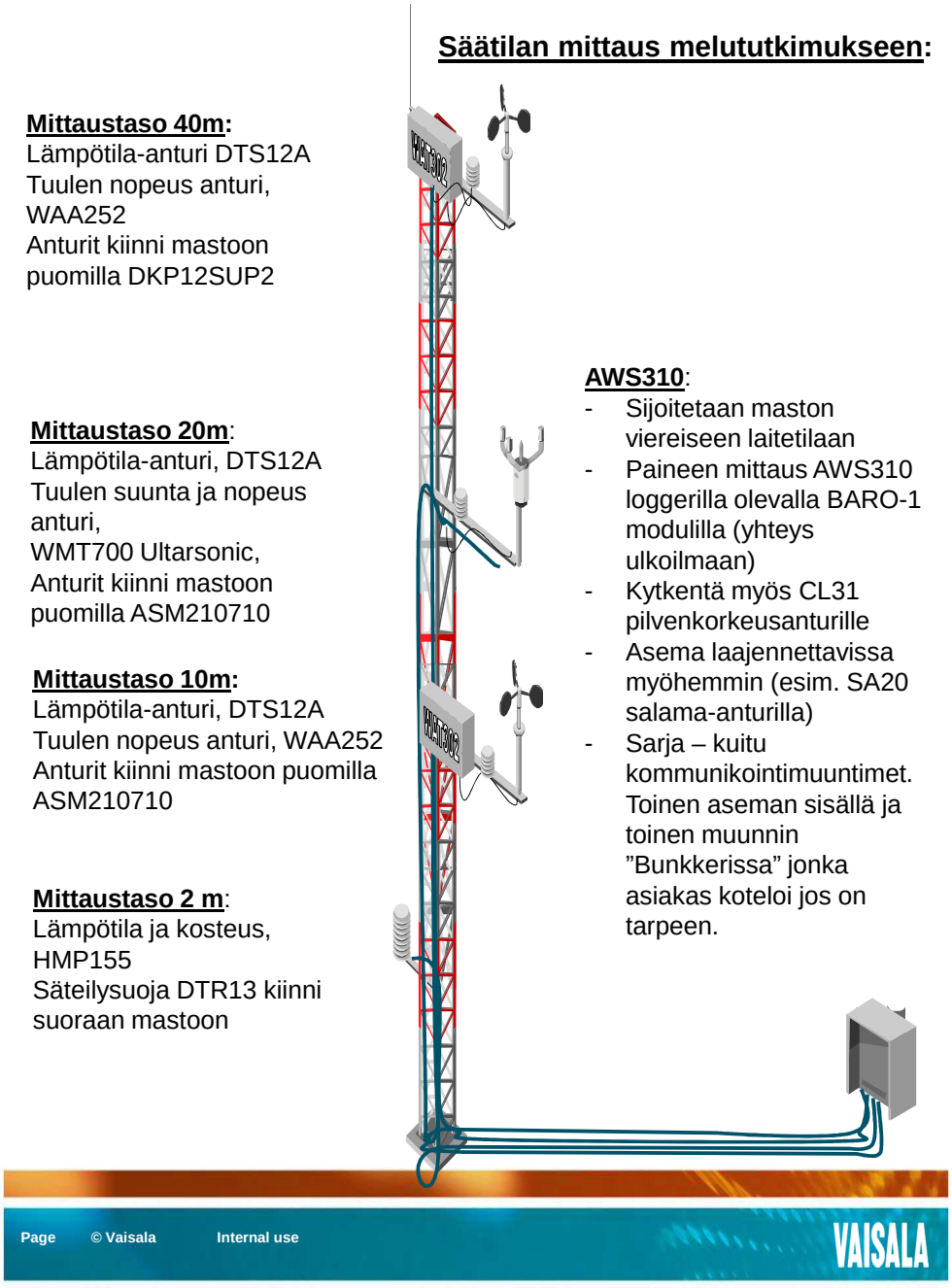

Figure B1: Meteorological station in Ähtäri site.The figure illustrates the sensor installation levels and models.

C Illustration of the terrain model in CadnaA

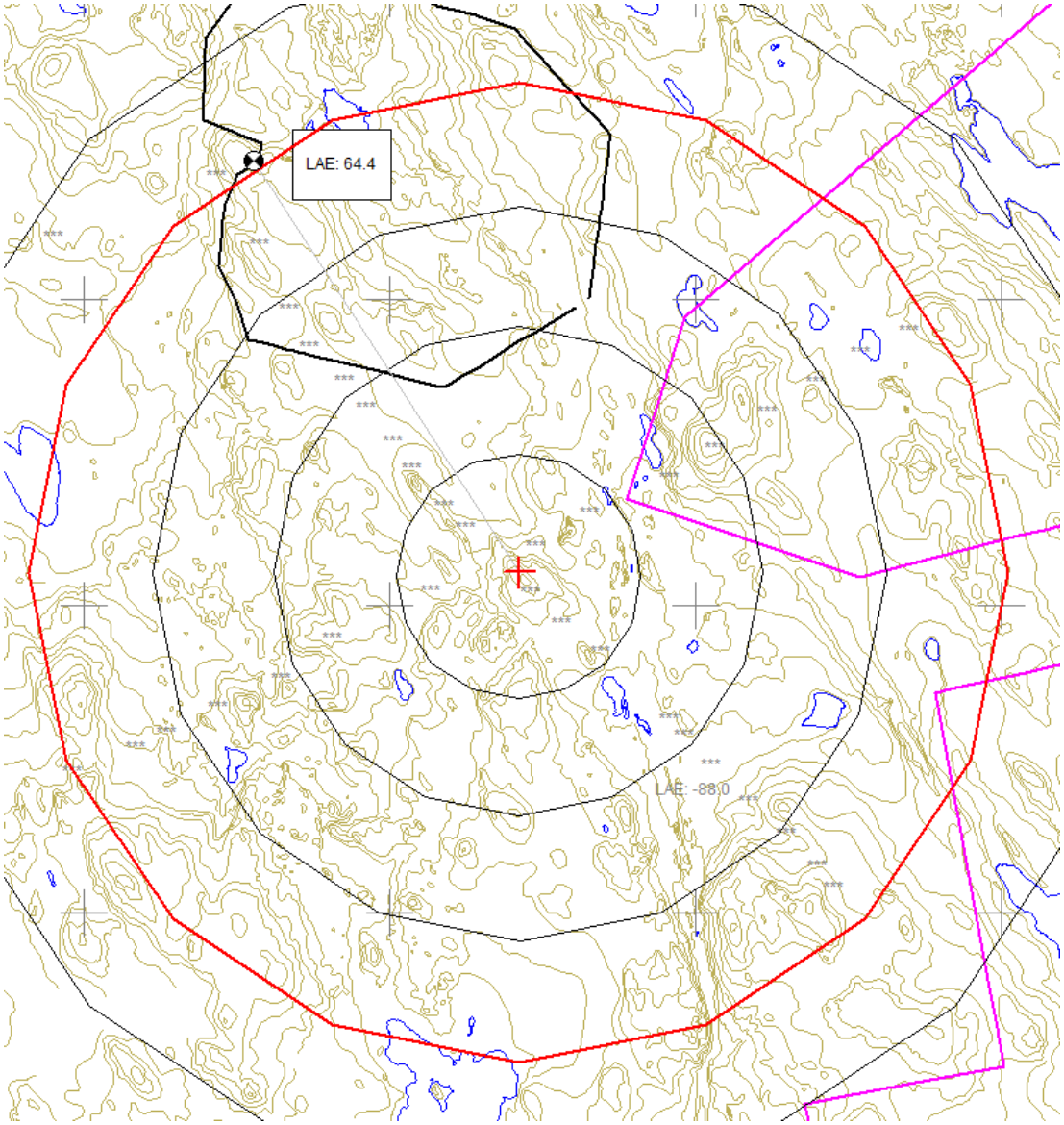

Figure C1: The terrain model used in the prediction software. Red cross in the center of the figure illustrates the sound source, and the receiver is marked with a black and white circle in the upper left quarter. Distance from the source is illustrated with circular lines (at interval of 1km) in the map. Contour line spacing is 2.5 meters. The map is taken from National Land Survey of Finland (Maanmittauslaitos).